Manuscript Details

Manuscript number	THESCI_2016_958
Title	Optimizing Microfluidic Separation Processes By Thermodiffusion Effect
Article type	Research Paper

Abstract

The numerical and experimental results presented in this work shows that a relatively small temperature gradient (5K), has great potential to generate a separation in interesting mixtures for biological purpose. In fact, it improves molecular diffusion separation process of a protective cryo (10% of dimethyl sulfoxide (DMSO) in phosphate buffered saline (PBS)) for cryopreserved cells, by 10%. This separation process was analyzed both numerically and experimentally, for which it was necessary to determine experimentally the thermophysical and transport properties of the mixture of 10% of DMSO in PBS. Experimental tests were done in a microdevice with a working section of 500µm x 25mm and a length of 75mm, which was designed, constructed and first of all validated with the mixture of reference H2O-Isopropanol at a mass fraction of 50%. Experimental test with the protective cryo were done with inflow rates between 1000 µL/ min to 4000 µL /min. The results confirm that the effect of thermodiffusion must be considered in handling processes of biological fluid mixtures because the existence of a thermal gradient could improve the efficiency of the separation process in microdevices.

Keywords	Microfluidics; Transport properties; Thermodiffusion; Biotechnology.

Corresponding Author	M. Mounir Bou-Ali
Corresponding Author's Institution	Engineering Faculty of Mondragon Unibertsitatea
Order of Authors	Alain Martin-Mayor, M. Mounir Bou-Ali, Maialen Aginagalde, Pedro Urteaga

Submission Files Included in this PDF

File Name [File Type]

Alain Martin-Mayor et al._2016.doc [Manuscript File]

GraphicAbstract.tif [Graphical Abstract]

Fig1.tif [Figure]

Fig2.tif [Figure]

Fig3a.tif [Figure]

Fig3b.tif [Figure]

Fig4a.tif [Figure]

Fig4b.tif [Figure]

Fig4c.tif [Figure]

Fig5.tif [Figure]

Fig6.tif [Figure]

Fig7a.tif [Figure]

Fig7b.tif [Figure]

Fig7c.tif [Figure]

Fig8.tif [Figure]

Fig9.tif [Figure]

fig10a.tif [Figure]

fig10b.tif [Figure]

fig10c.tif [Figure]

Fig11.tif [Figure]

Fig12.tif [Figure]

Fig13.tif [Figure]

Cover Letter_Alain Martin-Mayor et al._2016.doc [Cover Letter]

To view all the submission files, including those not included in the PDF, click on the manuscript title on your EVISE Homepage, then click 'Download zip file'.

Optimizing Microfluidic Separation Processes By Thermodiffusion Effect

Alain Martin-Mayor, M. Mounir Bou-Ali*, Maialen Aginagalde, Pedro Urtega

MGEP Mondragon Goi Eskola Politeknikoa, Mechanical and Industrial Manufacturing Department, Loramendi 4, Apdo. 23, 20500 Mondragon, Spain

* Corresponding author. Tel.: + 34 943794700 ext. 6312 Fax: +34 943791536

E-mail address: mbouali@mondragon.edu

Keywords: Microfluidics; Transport properties; Thermodiffusion; Biotechnology.

Abstract

The numerical and experimental results presented in this work shows that a relatively small temperature gradient (5K), has great potential to generate a separation in interesting mixtures for biological purpose. In fact, it improves molecular diffusion separation process of a protective cryo (10% of dimethyl sulfoxide (DMSO) in phosphate buffered saline (PBS)) for cryopreserved cells, by 10%. This separation process was analyzed both numerically and experimentally, for which it was necessary to determine experimentally the thermophysical and transport properties of the mixture of 10% of DMSO in PBS. Experimental tests were done in a microdevice with a working section of 500µm x 25mm and a length of 75mm, which was designed, constructed and first of all validated with the mixture of reference H2O-Isopropanol at a mass fraction of 50%. Experimental test with the protective cryo were done with inflow rates between 1000 µL/ min to 4000 µL /min. The results confirm that the effect of thermodiffusion must be considered in handling processes of biological fluid mixtures because the existence of a thermal gradient could improve the efficiency of the separation process in microdevices.

1. Introduction

For more than two decades, it has been considered that the miniaturization of test systems and procedures provide great advantage in diverse industries, particularly in the biotechnology sector [1]. This miniaturization requires the development of microfluidic platforms using a variety of devices in sample preparation, detection and diagnosis, mainly centered on the health sector. Many of these devices need efficient mixing and separation procedures, applied to molecules, analytes or particles [2]. As a result, in recent years, there have been countless numbers of new techniques and procedures developed for this determination [3, 4]. These techniques can be separated into two categories: i) passive devices, in which the separation or mixing operation is removed without the application of any external force, ii) active devices where actuators or external forces are employed for this goal.

Submillimeter dimensions of the channels used in microdevices, affects negatively in the operation of mixing or separation, because flows are purely laminar [5]. The absence of convection leads to do the mixing process under a purely diffusive regime. In order to optimize the mixing process in the majority of microdevices, T or Y geometries are used up as reference [6] [7] [8]. Similarly, chaotic advection has been used, which is based on breaking the laminar flow of sharp changes in geometry [9], or by introducing obstacles in the main channel in the form of poles [10] or grooves [11]. The possibility of improving mixing, forcing a transverse vortex called "Dean Flow" which introduces curvature in the main channel also has been studied [12], or applying acoustic fields [13], electric fields [14], magnetic fields [15] and others [16] [17].

Detection, quantification and analysis of clinical samples such as DNA, proteins or amino acids, require efficient separation processes, and several studies have attempted to develop such microtechnology [18]

[19]. Passive separation devices are used in applications involving the preparation of biological samples such as separation of blood plasma by capillary action [20], sedimentation [21] or the Zweifach -Fung effect [22]. For the extraction of different size analytes, filters were developed with H shape, where analytes are extracted due to the molecular diffusion coefficient difference [23]. Hydrodynamic forces have also been used for the separation of particles to control the entry conditions in curved channels [24], and straight channels [25]. The development of active microseparators has employed centrifugal [26], ultrasonic [27], electrical [28] or magnetic fields [29]. The implementation of such devices increases efficiency, however, technical complexity makes it more difficult to integrate them into microfluidic platforms. This is why so many advances have been made in passive separation, although it is inefficient and very complex [30].

Active devices, even if they are for mixing or separation, are more effective than passives. However this technology is more complicated to embed to the microdevices and to control them. That is why is doing great effort in passive devices to increase the efficiency up to the active ones in mixing and separation processes [30].

One of the applications of microfluidic devices is cleaning cryopreserved cells, which involves removing the protective cryo by molecular diffusion [31] [32]. Such these protective cryo is dimethyl sulfoxide (DMSO), which is mixed with PBS (phosphate buffered saline), used to cryogenate cells, tissues or organs [33]. Although DMSO protects the cell in freezing, exposure for a prolonged period have adverse impact on the cells [34] [35].Therefor, , cleaning is necessary before clinical application. The standard technique is the spin cleaning, however, this process may damage up to 30% of the cells [36]. This makes microdevices an attractive alternative..

Nevertherless, microdevices utilized for extracting cells DMSO from cells may have limited applicability because separation by molecular diffusion may be excessively slow. This study offers an experimental and numerical study in microdevices in order to optimize the separation efficiency of biological fluids using thermodiffusion effect by applying temperature gradients [37].

Thermodiffusion in liquids has been extensively examined [38], since it was discovered that a temperature gradient generates a redistribution of species in a mixture [39]. Later and independently, Soret quantified this in greater depth [39]; this is why the phenomenon of thermal diffusion is also called as Ludwing-Soret effect. The Ludwing-soret effect was an important development as it enabled the analysis of the partial separation of components in a mixture by the application of a temperature gradient. This phenomenon has great of importance in many natural processes, such as in the dispersion of components of oil wells [41] [42], or the dispersion of the components in the magma [43], in the characterization of isotopes [44], even in the distribution of elements in creating life [45] and also in biological fluids such as DNA, proteins or bacteria [46] [47] [48].

The result of a temperature gradient of a binary mixture generates a species flow according to Equation (1):

$$J = -D\nabla c_0 \rho - \rho D_T c_0 (1 - c_0)\nabla T \quad (1)$$

Where D is the molecular diffusion coefficient, c_0 is the mass fraction of the reference component in the initial homogeneous mixture, ρ is the density, D_T is the thermodiffusion coefficient and ∇T is the temperature gradient applied. The second term of Equation (1) quantifies the flow separation created by the temperature gradient within a mixture, which is governed by the thermodiffusion coefficient,. The first term, quantifies the mixture flow caused by concentration gradient, which is dominated by the molecular diffusion coefficient. When the denser component is led to the cold wall is called positive Soret effect, and the opposite is called negative Soret effect. Therefore, in order to understand the behavior of a mixture under the temperature gradient it is essential to quantify the value and the sign of the Soret coefficient. This is why the magnitude and sign can vary for the same mixture as a function of the concentration [49], average temperature [50], or even colloidal size [51].

This paper is organized into five parts. The beginning identifies the methodology used in the determination of thermophysical and transport properties. The following section shows the numerical model and the experimental validation. In the and discussion, the obtained optimization is checked in the procedure of separation by using temperature gradients. Finally, the conclusions are presented.

2. Determination of thermophysical and transport properties for DMSO/PBS mixture with a mass fraction of 10% of DMSO.

2.1. Thermodiffusion coefficient

To determine the mass flow generated within a mixture under the temperature gradient it is essential to know D_T and D. In order to determine experimentally D_T the Thermogravitational column technique in a flat configuration has been used (Fig. 1):

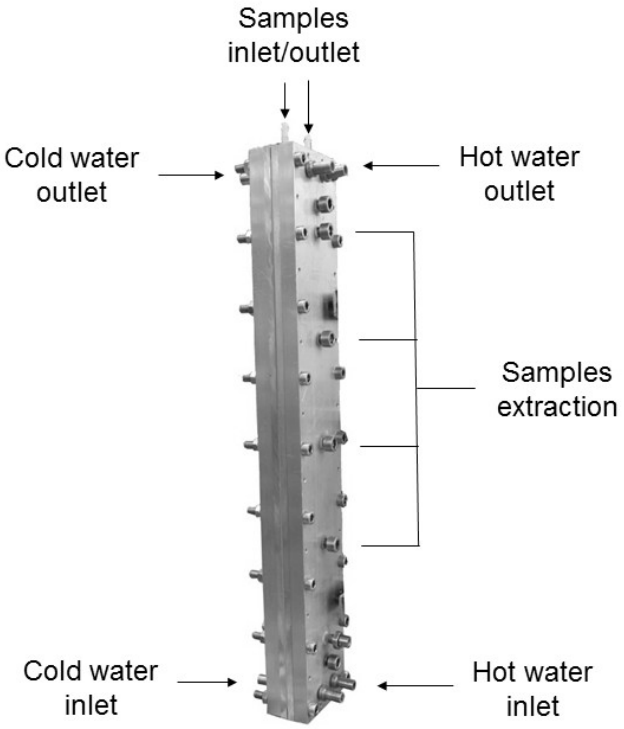

Fig. 1 Thermogravitational column (dimensions of the inner gap: 1mm x 50mm x 500mm)

The mixture is confined inside the gap and subjected to a horizontal temperature gradient. This temperature gradient is achieved by two tempered recirculating baths at $T_0+\Delta T/2$ and $T_0-\Delta T/2$ in each wall. The temperature gradient causes a horizontal separation of the mixture components inside the thermogravitational column (CT). The gravitational field effect enforced convection , thus generating a vertical separation. The Thermodiffusion coefficient can be determined once the solution reaches steady state using the FJO theory from the segregation by equation (2) [52] [53]:

$$D_T = - \frac{g L_x^4}{504} \frac{\alpha}{c_0(1 - c_0)\beta\mu} \frac{\partial\rho}{\partial z} \qquad (2)$$

Where μ is the dynamic viscosity, L_x is the inner gap of the CT, $\alpha = - (1/\rho) (\partial\rho/ \partial T)$ is the thermal expansion coefficient, $\beta = (1/\rho) (\partial\rho/ \partial c)$ is the mass expansion coefficient and g is the gravitational acceleration.

In this experiment the density gradient $\partial\rho/ \partial z$ was obtained by measuring the density of the extracted samples (4 in total) at different heights in the column, once the equilibrium state was reached (Fig. 2).

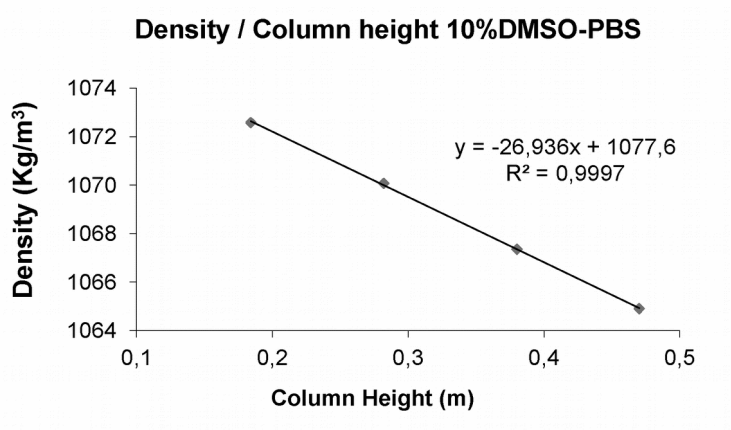

Fig. 2 Density in function of the height of the TC in the steady state, for a mixture of DMSO/PBS to a mass fraction of 10% DMSO at 25 ºC.

In order to obtain the mass expansion, a calibration of the density in function of the concentration was carried out. For this, different samples with a concentration in average of 25ºC, higher and lower than average concentration were used (Fig. 3a). Similarly, the thermal expansion coefficient was determined measuring the density of the mixture in function of the temperature (Fig. 3b). To determine these coefficients, the density was obtained by an Anton Paar densitometer DMA 5000 vibrating U quartz tube with a resolution of 1.10^{-6} g/cm^3, and with temperature control based on a Peltier system with a resolution of 0.001 K..

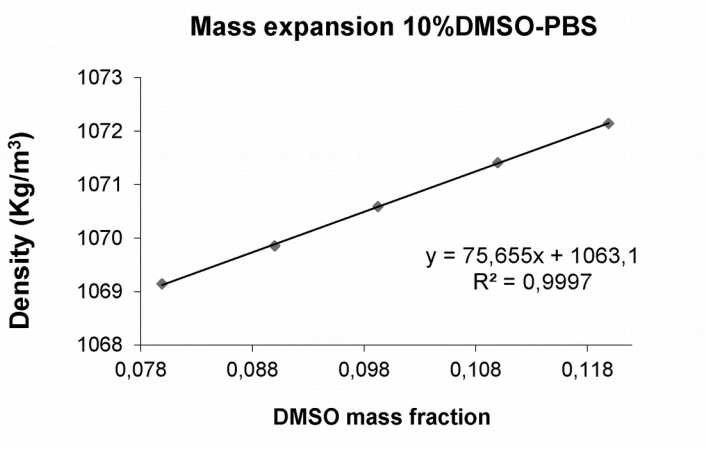

a)

b)

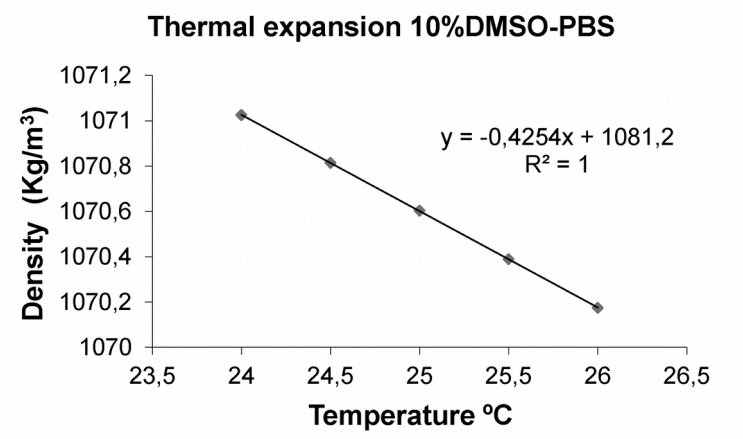

Fig. 3 Determination of a) mass and b) thermal expansion coefficient for the DMSO/PBS mixture to a mass fraction of 10% DMSO at 25 ºC

The viscosity was determined by an Anton Paar ball drop AMVn Microviscosimeter, the accuracy of which is ± 0.5%. Peltier elements integrated in the device control the temperature to an accuracy of 0.05 °C. A complementary method was also used; a HAAKE brand ball drop viscometer, which resolution is ± 1%.

1.1. Molecular diffusion coefficient

The determination of the molecular diffusion coefficient was been determined with the Sliding Symetric Tubes (SST) technique (Fig. 4). This technique requires a number of sets consisting of two identical tubes. These assemblies have two positions: separate (Fig. 4a) and facing tubes (Fig. 4b).

In the separate configuration, the contents of both tubes are separated, while in the position of facing tubes, the two tubes are tied. In the separate tubes, the mixture is inserted with a small concentration difference into each of the tubes.

To define the molecular diffusion coefficient of DMSO/PBS mixture (phosphate buffered saline) at 10% of DMSO, samples were prepared with 13% mass fraction of DMSO and another sample at 7% concentration of DMSO mass. The mixture with a higher density was introduced into the bottom tube, while the less dense mixture is inserted into the upper tube, thus preventing convection.

The sets were placed in separate tubes position in a bath at 25 °C (Fig. 4 c). In the separate position the mixtures are kept apart until the constant temperature is reached, then they are aligned (facing position) to allow the fluids to mix.

At different time intervals each set were changed to the separate tubes position, thus stopping diffusion. The change in concentration in each tube was determined in function of time, and therefore the molecular diffusion coefficient of the mixing was obtained [54] from the following equation:

$$\overline{w^{top}(t)} = \frac{1}{L}\int_{L}^{2L} w(z,t)dz = \frac{w^{top} + w^{bot}}{2} + \frac{4\left(w^{top} - w^{bot}\right)}{\pi^2}\sum_{n=0}^{\infty}\frac{e^{-\left(\frac{2n+1}{2}\right)^2\left(\frac{\pi}{L}\right)^2 D}}{(2n+1)^2}$$

$$\overline{w^{bot}(t)} = \frac{1}{L}\int_{0}^{L} w(z,t)dz = \frac{w^{top} + w^{bot}}{2} - \frac{4\left(w^{top} - w^{bot}\right)}{\pi^2}\sum_{n=0}^{\infty}\frac{e^{-\left(\frac{2n+1}{2}\right)^2\left(\frac{\pi}{L}\right)^2 D}}{(2n+1)^2} \quad (3)$$

Where w^{top} and w^{bot} represent the mass fraction in the upper and lower tube and L the length of the tube.

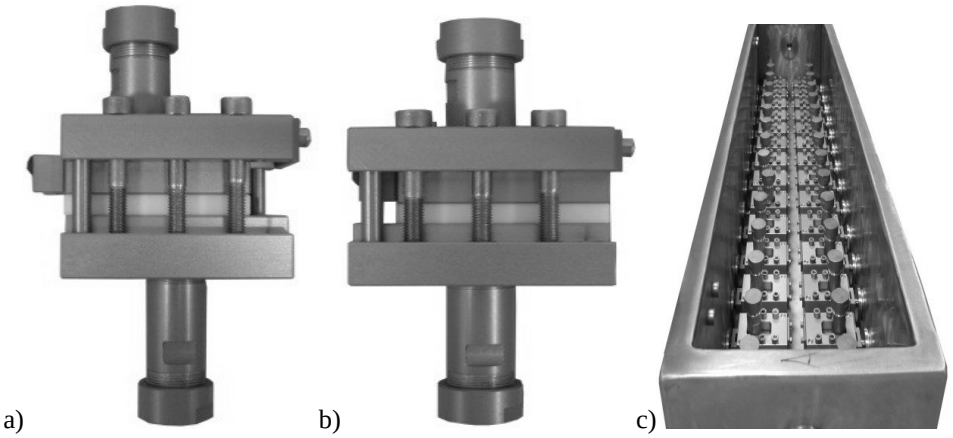

Fig. 4 The installation of Sliding Symmetric Tubes. a) Separate and b) facing tubes c) tempering bath with multiple sets SST

2.3. Results of thermosphysical and transport properties

Thermophysical and transport properties were specified for a mass concentration of 10% DMSO in PBS at 25 °C. Specifically the density, dynamic viscosity, thermal and mass expansion coefficient, thermodiffusion, molecular diffusion and Soret coefficient were determined. All experiments were replicated at least 4 times. In all cases the deviation was less than 4% with regard to the Soret coefficient ($S_T = D_T / D$).

Table 1 summarizes the results of the thermophysical and transport properties. This experimental study demonstrated that in the mixture, DMSO/PBS at 10% of DMSO and at a mean temperature of 25°C, the thermodiffusion coefficient is positive. Thus, in a temperature gradient DMSO, as DMSO is the heaviest component, it concentrates or migrates to the cooler wall.

Table 1 Transport and thermophysical properties of DMSO/PBS mixture at 25 °C and a mass fraction of 10% DMSO

DMSO	ρ *(kg/m³)*	*μ (mPa·s)*	*β (10⁻¹)*	*α (10⁻³) (K⁻¹)*	*D (10⁻⁹) (m²/s)*	*D_T (10⁻¹¹) (m²/K·s)*	*S_T (10⁻³)(K⁻¹)*
10%	1070.64	1.345	0.706	0.397	1.88	2.38	1,26

3. Numerical model

The numerical studies carried out in this report are based on the Finite Volume Method (FVM) and Computational Fluid Dynamics (CFD) [55]. The separation process with the thermodiffusion effect in the microdevice employed by Mata *et. al.* [32] was numerically analyzed to separate DMSO. The microdevice consists mainly of a central cavity of constant rectangular section in which separation occurs. The flows are introduced through two opposite inputs. These two streams are separated by a divider plate that redirects the flow and prevents mixing between them at the inlet, so that they flow in parallel through the central cavity in laminar regime. Flow extraction is done by two outputs identical to the input pattern. The total length from the inputs to the outputs is L = 125 mm. The input splitter allows achieving fully developed parabolic flow in the inlet of the central cavity. In contrast the output splitter is to obtain undisturbed sampling.

In this study, the cleaning fluid (PBS) was introduced in the upper inlet. A mixture of 10% of DMSO in PBS was introduced in the lower inlet. The model used in the numerical simulation represents the principal components of the device, the central cavity and the changeover to the entryway and exit (Fig. 5).
The central cavity consists of two flat plates which creates a constant rectangular gap. The dimensions are exactly the same as those used by Mata *et al.* [32], 25 mm wide, 500 µm high and 75 mm long.

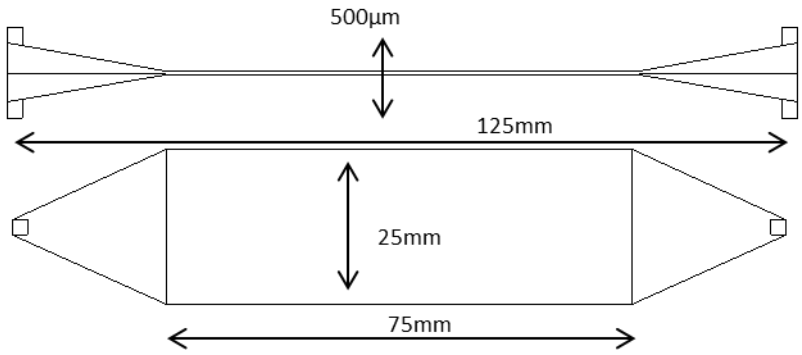

Fig. 5 Model used for the numerical study

A 3D implicit numerical method was used assuming incompressible laminar flow at atmospheric pressure. In order to obtain accurate results the double precision method was used. To prevent instabilities, second-order discretization of pressure, density, velocity, mass and energy was applied. The residual convergence criterion was established by an order of magnitude of 10^{-14}. This ensured a convergence of the values. Gambit software [56] was used for 3D pre-procesing the computational domain of which was composed of a grid unevenly spaced of hexaedral cells To have a realistic representation of the concentration gradients, a very fine mesh resolution of 1125000 cells was made.

The model fulfills Fick molecular diffusion low and thermodiffusion model The alterations in fluid density with the concentration and temperature are expresed by the Boussinesq approximation, as described in equation (4) [57]:

$$\rho = \rho_0 (1 + \alpha(T - T_0) + \beta(c - c_0)) \quad (4)$$

Where ρ is the density in each cell, ρ_0 is the density of the homogeneous mixture, T the temperature in each cell and T_0 is the average temperature.

Mass transport is described by the equation (1). The temperature difference applied between the upper and lower walls of the central cavity is 5 K. A "non –slip" boundary condition was imposed on the walls.

3.1. Validation of the numerical model

In order to validate the numerical model the results of separation obtained [32] for different working conditions [37] in the purely diffusive regime were analyzed. In order to apply numerical analysis the transport and thermophysical properties of the mixture were determined and are presented in Table 1.

The results for the 16 cases analyzed are shown in Table 2, which represents the dimensionless dependent variable concentration in the bottom outlet c_c/c_0 where c_0 is the initial mass concentration of DMSO (10%) and c_c is the mass of DMSO concentration in the exit. Furthermore, it represents the proportion between the input streams, according to equation (5):

$$f_q = \frac{Q_{DMSO - PBS}}{Q_{TOT}} \quad (5)$$

Where $Q_{DMSO-PBS}$ is the volumetric flow rate off the DMSO/PBS mixture to a mass fraction of 10% of DMSO (bottom inlet) and Q_{TOT} is the total inlet volumetric flow rate. The PBS inlet flow is Q_{PBS} (upper inlet), thus $Q_{TOT} = Q_{PBS} + Q_{DMSO-PBS}$.

Table 2 Comparison of experimental and numerical separation ratio in a **purely diffusive regime, for the mixture of DMSO/PBS with a mass fraction of 10% DMSO at a mean temperature of 25 °C**

f_q	^{QTO}T *(10^{-8}) (m^3/min)*	c_c/c_0 [30]	c_c/c_0 (this work)	deviation *(%)*
0.1	3.3	0.13	0.132	1.53
0.1	5.4	0.17	0.173	1.76
0.1	7.5	0.20	0.202	1
0.1	13.3	0.26	0.257	-1.15
0.15	3.3	0.20	0.204	2
0.15	5.4	0.25	0.255	2
0.15	7.5	0.29	0.296	2.06
0.15	13.3	0.37	0.373	0.81
0.23	3.3	0.30	0.304	1.33
0.23	5.4	0.36	0.373	3.6
0.23	7.5	0.41	0.426	3.9

0.23	13.3	0.52	0.524	0.77
0.37	3.3	0.46	0.457	-0.65
0.37	5.4	0.53	0.534	0.75
0.37	7.5	0.59	0.591	0.17
0.37	13.3	0.69	0.689	-0.15

Fig. 6 shows the results of the dimensionless variable depending on c_c/c_0 in function of Reynolds number (Re). These variables are parameterized by f_q, where the experimental results of [32] are compared with those obtained numerically in this work. The correlation between the results validated the developed model which accurately reproduces the separation behavior in the purely diffusive regime.

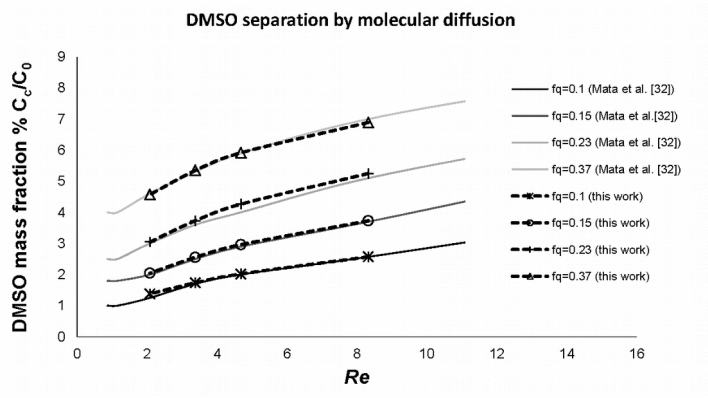

Fig. 6 Extraction fraction of DMSO c_c/c_0 in function of Reynolds with the cell geometry of Fig. 5.

4. Flow Facility and Experimental Methods

Flow Device

The device for the experimental study of the thermodiffusion effect in the separation of DMSO, was built in aluminum. The upper and lower cavity are of identical geometry, where the same geometry to that employed in the numerical model was obtained. For the generating of the temperature gradient, outside upper and lower cavity was machined were hot and cold water can flow. To avoid inside velocity grandients of the mixture, the cross section area must be the same through the device, thus 2.85mm diameter bottom inlet/outlet and upper inlet/ outlet holes were drilled. The gap from where the mixture will flow, was generated by a 500µm polyetheretherketone (PEEK) sheet, which has a high chemical stability and low conductivity and thermal expansion [58] [59]. The entire internal cavity has polished with a paste of 1 micron diamond dust (STRUERS, DP -Paste M) to achieve the lowest surface rugosity as possible.

Two bottom and top holes were made where a resistance temperature detector (RTD) PT100 probe can be introduced as closes as possible form the gap (at 1 mm from the gap), in order to measure the temperature

gradient between the upper and bottom walls at the entrance and exit of the central cavity. In order to generate the thermal gradient two thermostatically tempered baths (Proline RP- 855) was used.

To achieve the tightest of all the elements, viton O ring has been used. Fig. 7 shows the complete assembly of the constructed microdevice (Fig. 7a) and the inner details of the same (Fig. 7 b and c).

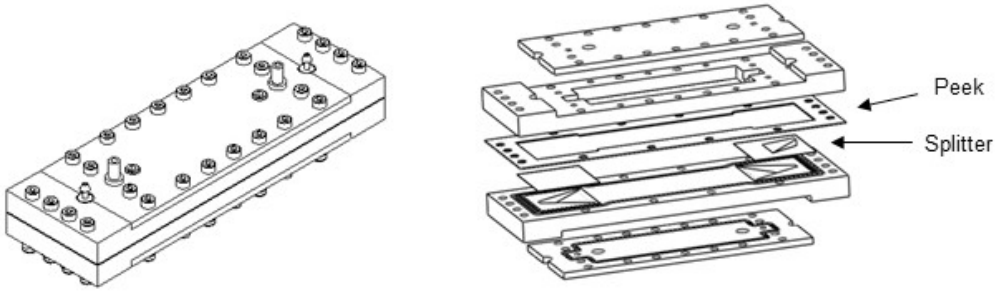

a) b)

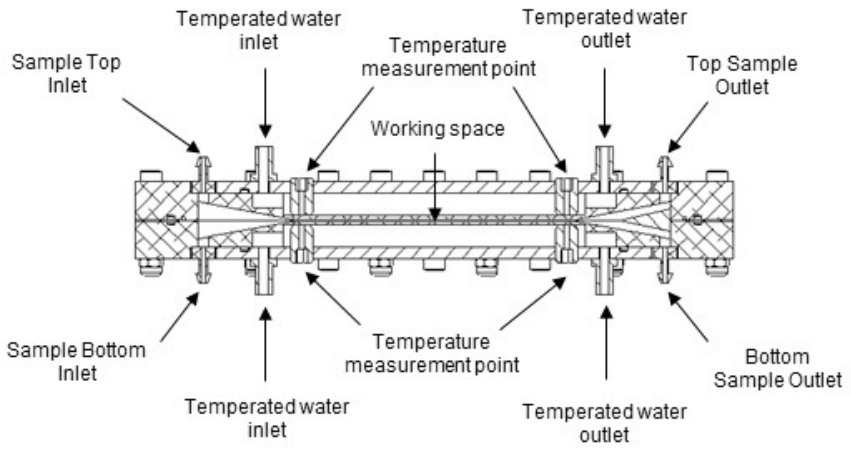

c)

Fig. 7 Design of the experimental device a) assembled device b) device exploded c) central cut of the device

1.2. Flow rate control and measurement

Flow was controlled by a MFCS-8C-1000mbar (Microfluidic Control System) and Flowell-1000µL/min device with the Maesflow software from the Fluigent company. The first, deals with the control of pressure with a resolution of 1mbar and a maximum pressure of 1034 mbar. The pressure control is performed in both, inputs and outputs. The Flowell-1000µL/min is responsible for controlling the flow. It has three flowmeters, so the control of all inputs and outputs is guaranteed. The maximum flow measured is 1000 µL/ min with a resolution of 0.1 µL/ min, with a ± 5% error. Outlet samples mass fraction was

analyzed using the Anton Paar DMA 5000 densimeter. Fig. 8 shows a diagram of the experimental measurement system.

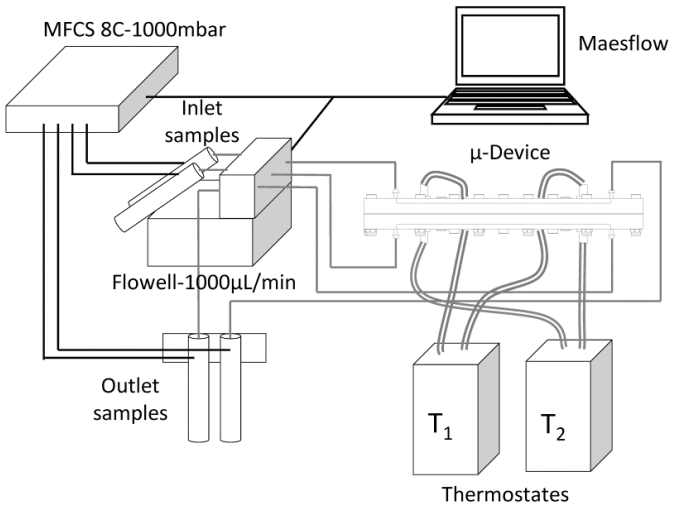

Fig. 8 Scheme of the experimental measurement

5. Flow device characterization

For the experimental validation of the device, the results of a standard mixture were studied in the purely diffusive regime. The reference mixture was H_2O/Isopropanol to a mass fraction of 50%, which thermophysical and transport properties are known and are well studied in the literature. Table 3 summarizes the properties in order to carry out the experimental verification [60].

Table 3 Thermophysical and transport properties of H_2O/Isopropanol mixture at a mass fraction of 50% and at 25 ºC

H_2O	ρ (kg/m^3)	μ $(mPa{\cdot}s)$	β	α (10^{-3}) (K^{-1})	D (10^{-10}) (m^2/s)
50%	902,37	3,055	0,2606	0,9004	1,68

The molecular diffusion evolution of the mixture was analyzed in function of the flow rate. For this purpose and taking into account that the denser component in the mixture of water/isopropanol is the water, through the lower entrance was introducted a mixture of 53% of water, and through the top entrance, 47% of water. This avoids internal instabilities due to the convection. The flow range of each entry was 50 µl/min to 1000 µl/ min, where the flow of both inputs was the same. Tests were conducted at 25 °C temperature. To define the characteristics of the samples at the output, the method of analysis based on the measurement of density was employed.

A total of 10 cases of different flow rates have been analyzed, Fig. 9 depicts the results obtained.

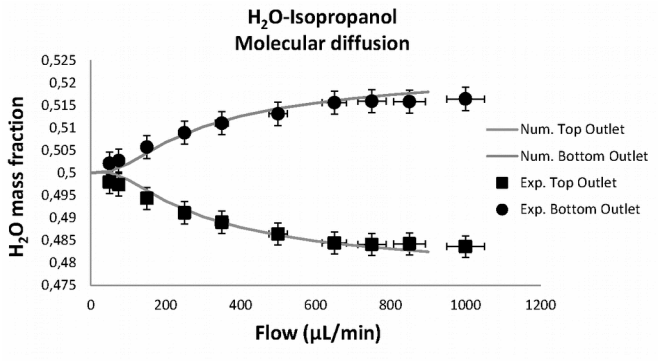

Fig. 9 Comparison between experimental and numerical results of the H2O/isopropanol mixture by molecular diffusion in function of the flow rate at 25 °C

The dashed line represents the numerical results of the concentration of H_2O in the upper outlet, and the solid line, the results of the lower output. The filled square symbols represent the experimental data of the concentration of the upper outlet and the circles the lower output data for each inflow rate. As shown in Fig. 9, as the inflow rate is decreased, the top and bottom outlet H_2O concentration get closer because the mixture has more time to mix due to the molecular diffusion. Finally, at inflow rate close to 50 µl/min, top and bottom outlet H_2O mass fraction concentration is of 0.5, which denotes that the mixture is completely mixed. As shown in Fig. 9, the good agreement between the experimental and numerical results validated experimental device operation.

5. Results and discussion

Once validated numerically and experimentally the microdevice, the analysis of the degree of separation of DMSO/ PBS mixture with and without temperature gradient is done.

In order to analyze the thermodynamic behavior of the mixture in the microdevice, it was essential to determine the thermophysical and transport properties of the DMSO/PBS mixture of a mass fraction of 10% DMSO (Table 1). The Table 1 shows, the sign of the thermodiffusion coefficient in the analyzed mixture is positive, which means a positive Soret behavior. Thus, the denser component of the mixture, DMSO, was be attracted to the cooler wall.

First, the behavior of the mixture was analyzed only in the diffusive regime at 25 °C (without temperature gradient). To carry out this experiment various conditions at different inflow rates in the entrances were investigated; f_q =0,4, f_q=0,5 and f_q=0,6. Thus, a 40 % of the total inflow was introduced in the bottom inlet for the case f_q =0,4, 50% for the case f_q =0,5 and 60% for the case f_q =0,6, where from the botton inlet the mixture of DMSO/PBS at a mass fraction of 10% of DMSO is introduced and from the top inlet PBS.

Fig. 10 compares the experimental and the numerical results, where the mass fraction of DMSO is represented in the top and bottom outlet, in terms of the full flow rate. Horizontal error bars correspond to the measurement error of the flowmeter, which in the worst case was 5%, while the vertical error

corresponds to the difference between the results obtained in several trials, which in worst cases was less than 6%.

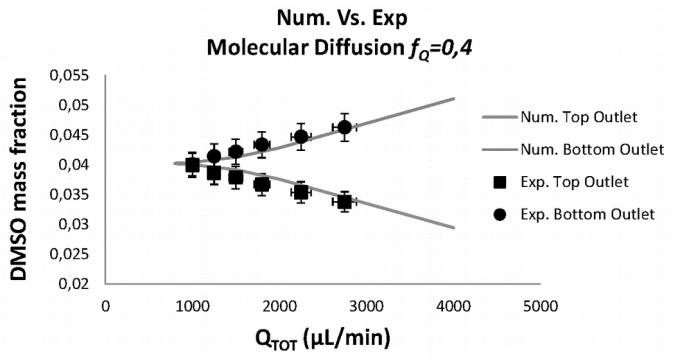

a)

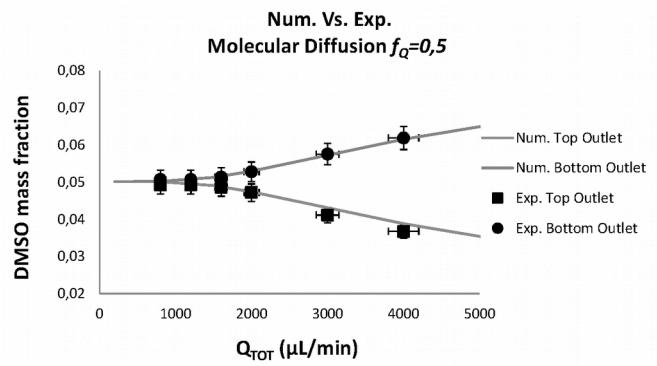

b)

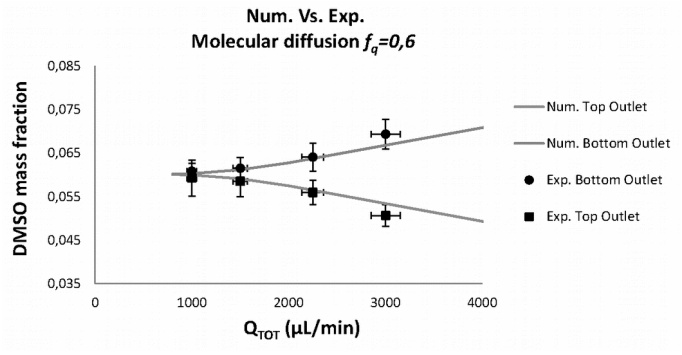

c)

Fig. 10 Comparison of the molecular diffusion separation of DMSO represented as mass fraction of DMSO to the outputs depending on the total flow. Cases a) f_q =0,4, b) f_q =0,5 y c) f_q =0,6

As shown in Fig. 10, the behavior of the mixing process of DMSO is similar to the one explained for the case of H_2O-Isopropanol (Fig. 9). So, as the inflow rate decreases, the top and bottom outlet DMSO concentration get closer to the full mixed concentration, what happens close to 1000 µL/min. For the case of f_q =0,4, (Fig. 10 a) this corresponds to a mass fraction of DMSO of 0.04, for f_q =0,5, (Fig. 10 b) to 0.05 and for f_q =0,6, (Fig. 10 c) to 0.06. This is the maximum DMSO that can be separated by molecular diffusion (without a temperature gradient) for each case. So, if for all cases the inlet DMSO concentration of the mixture of interest (bottom inlet mixture), is of 10%, the outlet DMSO concentration of the mixture

of interest (bottom outlet) is of 4% for the case f_q =0,4, 5% for the case f_q =0,5 and 6% for the case of f_q =0,6.

The full mixing point of these three cases is much faster (around Q_{TOT}= 1000 µL/min, Fig. 10) than for the case of H_2O-Isopropanol (around Q_{TOT}= 75 µL/min, Fig. 9). This is natural as the diffusion coefficient of the mixture of H_2O-Isopropanol is one order of magnitude smaller than the one of the mixture DMSO/PBS (see Table 1 and Table 3).

Analyzing the results shown in Fig. 10, can be concluded that the numerical and experimental results are in good agreement. It was observed that the maximum extraction ability of DMSO in each case is determined by the input flows ratios. The lowest concentration of DMSO in the output was directly proportional to f_q. These results confirm those obtained by Mata *et al.* [32].

In order to determine the influence of the temperature gradient on the extraction of DMSO, the case of the f_q =0,5 it was analyzed numerically and experimentally using a temperature gradient of 5 K. As for the cases analyzed in Fig. 10, from the bottom inlet the mixture of DMSO/PBS at a mass fraction of 10% of DMSO is introduced and from the top inlet PBS, at a Q_{TOT} up to 4000 µL/min.

Fig. 11 shows the numerical results comparison of the DMSO extraction with and without temperature gradient, where the dashed line represents the case of extraction by molecular diffusion (without temperature gradient), and the solid line represents the results with a temperature gradient. As explained before, the thermodiffusion coefficient for the mixture of 10% DMSO in PBS is positive as shown in Table 1. This means that the denser component (DMSO) will be attracted by the cooler wall. As the mixture of DMSO/PBS is introduced from the bottom inlet, to increase the extraction of DMSO, the upper wall is cooled and the lower wall is warmed, creating a temperature difference of 5 K, between a mean temperature of 25ºC.

For the case without temperature gradient and at an inflow of Q_{TOT} = 4000 µL/min, the top outlet DMSO mass fraction concentration is of 0.038 and the bottom outlet DMSO mass fraction concentration is of 0.062. As explained before, as the inlet Q_{TOT} decreases, the mass fraction of DMSO between top and bottom outlets gets closer (because the DMSO mixes by molecular diffusion), till a constant value of 0.05. This constant value of 0.05 is reached at an around intlet flow of Q_{TOT} = 1000 µL/min, and stays constant for lower values. This denoted that the mixture is fully mixed.

For the case with temperature grandient, and for the same inlet conditions, at an inflow of Q_{TOT} = 4000 µL/min, the topoutlet DMSO mass fraction concentration is of 0.042 and the bottom outlet DMSO mass fraction concentration is of 0.058. Comparing with the case without temperature gradient, for this case a higher extraction of DMSO is obtained (around 6.45% more) due to the Soret effect. In this case too, if the Q_{TOT} is decreased a value of 0.05 of DMSO mass fraction is obtained in both outlets. However, for the case with temperature gradient this value is obtained at a Q_{TOT} of 2000 µL/min (for the case without temperature gradient this happens at a Q_{TOT} = 1000 µL/min). So, using the Soret effect, a faster fully mixed mixture can be achieved if is compared to the case without temperature gradient (37.5 % faster). Moreover, for the case with temperature gradient, if the inflow rate used is smaller than 2000 µL/min, due

to the Soret effect, an increase of the DMSO separation ratio happens. For an inflow rate of 1000 µL/min, the top outlet DMSO mass fraction concentration is of 0.055 and the bottom is of 0.045. This means that using a temperature gradient a 10% higher separation of DMSO con be achieved compared without temperature gradient, due to the Soret Effect.

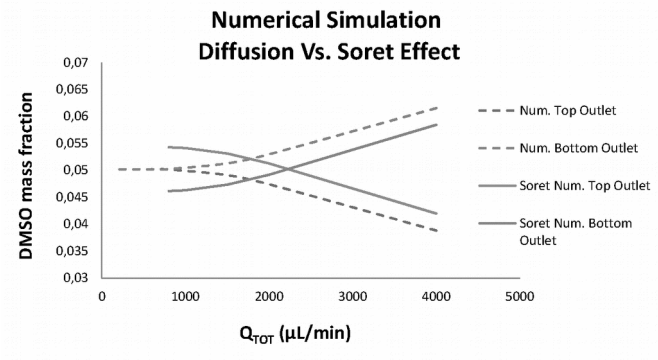

Fig. 11 Comparison of the mass fraction extracted at the upper and lower outputs, under the thermodiffusion effect, for the case f_q =0,5 at an average temperature of 25 ° C

From the numerical results obtained, the separation efficiency can be analyzed defining this as the percentage needed to achieve the homogeneous mixture [61]:

$$Extraction_{Efficiency} = 100 \cdot \frac{(c_0 - c_c)}{c_0} \tag{6}$$

In Fig. 12, the efficiency is represented as a function of the flow rate for the purely diffusive (without temperature gradient) and thermodiffusive (with temperature gradient) cases. As can be seen, while the case of the diffusive reaches its maximum efficiency at around 1000 µL / min, in the thermodiffusive case, this is reached at around 2250 µL/min. Therefore apart from obtaining a greater separation, a faster separation process can be achieved. To lower flow rates, the results indicate that the thermal effect enhances extraction of DMSO, obtaining extraction efficiency above 50%, and improving the process by 10%.

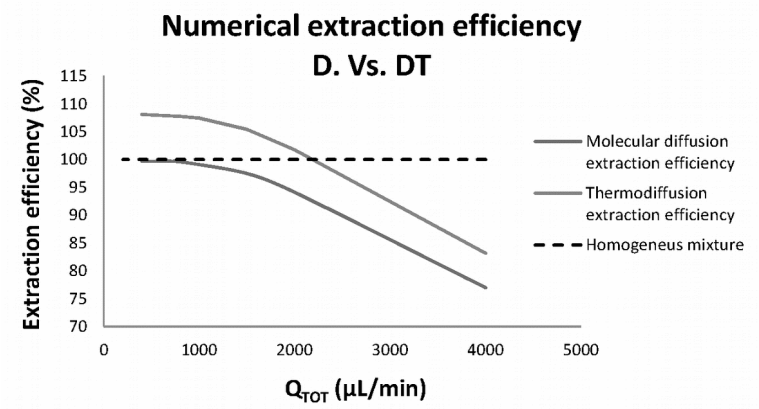

Fig. 12 The numerical results of the efficiency of DMSO extraction applying (molecular diffusion (gray dashed line), temperature gradient (continuous line) for f_q =0,5 at a mean temperature of 25 °C

The experimental results have been compared with those obtained numerically in the thermodiffusive regime and the behavior was test to be the same in both cases. Solid lines present the numerical results while solid circles and squares show the experimental outcomes. As observed in Fig. 13, he homogenization of the mixture occurred at higher flow rates in contrast to what was observed numerically. This variance may be made due to the estimate in the experimental determination of the thermodiffusion coefficient of the binary mixture, considering the PBS as a pure fluid in the thermogravitational column.

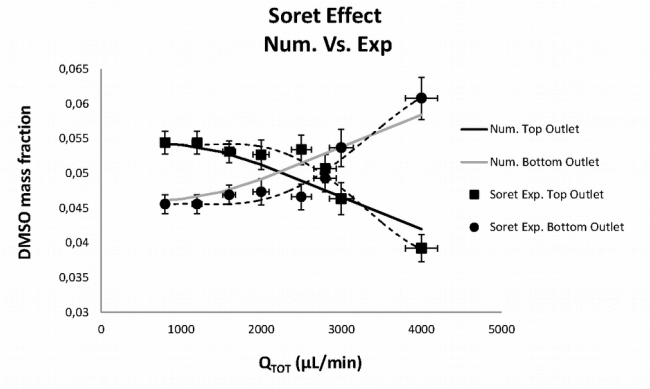

Fig. 13 Comparison of numerical and experimental studies of DMSO extraction in function of the total volume under the thermodiffusive effect. Dashes lines represent the numerical results while solid circles and squares show the experimental results

6. Conclusions

The results obtained in this study show that the effect of thermodiffusion, is not despicable phenomenon at submillimeter scale, as the order of action can become very influential in processes of mixing or separation of biological samples. It is demonstrated that a relatively small temperature gradient (5K), has potential to generate effective transport in biological mixtures, increasing 10% compared to the purely diffusive regime separation. The results confirm that the effect of thermodiffusion must be considered in biological fluids handling processes where the mix or separation plays an important role, since the existence of a temperature gradient could affect the efficiency. Thus, consideration of this effect could be key in applications at microscale where an active actuator becomes irretrievably in a heat source. So, knowing the sign and magnitude of the thermodiffusion coefficient of the sample of interest, together with the location of the heat source, it is essential to use the temperature gradient in beneficial way for the process.

7. Acknowledgements

The Mondragon Goi Eskola Politeknikoa (MGEP) group thanks TERDISOMEZ (No. FIS2014-58950+C2-I-P) project from the Spanish Government, as well as the MICROXOM (No. PI2014-1-70), Elkartek Proyect (MICRO4FAB) and the project of Fluids Mechanics Groups (IT1009-16) of the Basque Country Government.

8. References

[1] S. J. Lee. S. Y. Lee (2004) "Micro total analysis system (μ-TAS) in biotechnology", *Appl Microbiol Biotechnol.,* 64: 289–299.

[2] N. Pamme (2007)."Continuous flow separations in microfluidic devices", *Lab Chip*, 7: 1644–1659.

[3] L. Florea, A. Martin-Mayor, M. M. Bou-Ali, K. Meagher, D. Diamond, M. Tutar, F. Benito-Lopez (2016), "Adaptive coatings based on polyaniline for direct 2D observation ofdiffusion processes in microfluidic systems", *Sensors and Actuators B,* 231: 744–751.

[4] I. González, M. Tijero, A. Martin, V. Acosta, J. Berganzo, A. Castillejo, M. M. Bou-Ali and J. L. Soto (2015), "Optimizing Polymer Lab-on-Chip Platforms for Ultrasonic Manipulation: Influence of the Substrate", *Micromachines*, 6: 574-591.

[5] T. M. Squires, S. R. Quake (2005) "Microfluidics: Fluid physics at the nanoliter scale", *Rev. Mod. Phys.*, 77: 977-1026.

[6] A. E. Kamholz (1999) "Quantitative analysis of molecular interactive in microfluidic channel: the T-sensor" *Anal. Chem.*, 71: 5340–5347.

[7] A. E. Kamholz and Paul Yager (2001) "Theoretical analysis of molecular diffusion in pressure-driven laminar flow in microfluidic channels", *Biophys. J.,* 80: 155–160.

[8] R. F. Ismagilov (2000) "Experimental and theoretical scaling laws for transverse diffusive broadening in two-phase laminar flows in microchannels" *Appl. Phys. Lett.,* 76: 2376–2378.

[9] R. Vijayendran, K. Motsegood, D. Beebe, D. Leckband (2003) "Evaluation of a threedimensional micromixer in a surface-based biosensor", *Langmuir,* 19 (5): 1824–1828.

[10] A. Asgar, S. Bhagat, E. T. K. Peterson and I. Papautsky (2007)"A passive planar micromixer with obstructions for mixing at low Reynolds numbers", *J. Micromech. Microeng.*, 17: 1017–1024.

[11] T. Johnson, D. Ross, L. Locascio (2002) "Rapid microfluidic mixing", *Anal. Chem., 74*: 45-51 .

[12] F. Jiang, K. Drese, S. Hardt, M. Kupper, F. Schonfeld (2004) "Helical flows and chaotic mixing in curved micro channels". *AIChE J.*, 50 (9): 2297–2305.

[13] T. Luong, V. Phan, N. Nguyen (2011), "High-throughput micromixers based on acoustic streaming induced by surface acoustic wave", *Microfluid. Nanofluid*, 10: 619–625.

[14] M.Z. Huang, R.J. Yang, C.H. Tai, C.H. Tsai, L.M. Fu (2006) “Application of electrokinetic instability flow for enhanced micromixing in cross-shaped microchannel”, *Biomed. Microdevices*, 8: 309–315.

[15] Y. Wang, J. Zhe, B. T. F. Chung, P. Dutta, (2008) “A rapid magnetic particle driven micromixer”. *Microfluid. Nanofluid*, 4: 375–389.

[16] L. Capretto, W. Cheng, M. Hill and X. Zhang (2011) “Micromixing within microfluidic devices”, *Top. Curr. Chem*., 304: 27–68.

[17] N.T. Nguyen and Z. Wu (2005) “Micromixers—a review”, *J. Micromech. Microeng*. 15: 1–16.

[18] D. R. Gossett, W. M. Weaver, A. J. Mach, S. C. Hur, H. T. K. Tse, W. Lee, H. Amini, D. Di Carlo (2010) “Label-free cell separation and sorting in microfluidic systems”, *Anal. Bioanal. Chem*., 397: 3249–3267.

[19] C.H. Tai, S.K. Hsiung, C.Y. Chen, M.L. Tsai, G.B. Lee (2007) “Automatic microfluidic platform for cell separation and nucleus collection”, *Biomed Microdevices*, 9: 533–543.

[20] D. Kim, J. Y. Yun , S. J. Park, S. S. Lee (2009) “Effect of microstructure on blood cell clogging in blood separators based on capillary action”, *Microsys. Technol*., 15: 227–233.

[21] T. Tachi, N. Kaji, M. Tokeshi, B. Yoshinobu (2009) “Simultaneous separation, metering, and dilution of plasma from human whole blood in a microfluidic system”, *Anal.Chem.*, 81: 3194-3198.

[22] S. Yang, B., A. Undar, Jeffrey D., Zahn (2006) “A microfluidic device for continuous, real time blood plasm separation”, *Lab chip*, 6: 871-880.

[23] P. Yager, T. Edwards, E. Fu, Kristen Helton, Kjell Nelson, Milton R. Tam and Bernhard H. Weigl (2006) “Microfluidic diagnostic technologies for global public health”, *Nature*, 442: 412-418.

[24] S. S. Kuntaegowdanahalli, A. Asgar, S. Bhagat, G. Kumarb and I. Papautsky (2009) “Inertial microfluidics for continuous particle separation in spiral Microchannels”, *Lab Chip*, 9**:** 2973–2980.

[25] A. Asgar, S. Bhagat, S.S. Kuntaegowdanahalli, I. Papautsky (2009) “Inertial microfluidics for continuous particle filtration and extraction”, *Microfluid Nanofluid*, 7: 217–226.

[26] S. Haeberle, T. Brenner, R. Zengerle and J. Ducreé (2006) “Centrifugal extraction of plasma from whole blood on a rotating disk”, *Lab Chip*, 6: 776–781.

[27] I. González, L. J. Fernández, T. E. Gómez, J. Berganzo, J. L. Soto , A. Carrato (2010) “A polymeric chip for micromanipulation and particle sorting by acoustic fields based on a multilayer configuration”, *Sens. Actuators B*, 144: 310-317.

[28] M. T. Badal, M. Wong, N. Chiem, H. Salimi-Moosavi, D. J. Harison (2002) “Protein separation and surfactant control of electroosmotic flow in poly(dimethylsiloxane) coated capillaries and microchips”, *J Chromatogr A*, 947: 277–286.

[29] N. Xia, T. P. Hunt, B. T. Mayers, E. Alsberg, G. M. Whitesides, R. M. Westervelt, D. E. Ingber (2006) “Combined microfluidic-micromagnetic separation of living cells in continuous flow”, *Biomed. Microdevices*, 8: 299–308.

[30] D. Di Carlo, D. Irimia, R. G. Tompkins (2007) “Continuous inertial focusing, ordering, and separation of particles in microchannels”, *PNAS*, 104: 18892–18897.

[31] K.K. Fleming, E.K. Longmire, A. Hubel (2007) “Numerical characterization of diffusion-based extraction in cell-laden flow through a microfluidic channel”, *J. Biomech. Eng.*, 129: 703–711.

[32] C. Mata, E.K. Longmire, D.H. McKenna, K.K. Glass, A. Hubel (2008) “Experimental study of diffusion-based extraction from a cell suspension”, *Microfluid Nanofluid*, 5: 529–540.

[33] A. Torreggiani, M. Di Foggia, I. Manco, S.A. Markarian, S. Bonora (2008) “Effect of sulfoxides on the thermal denaturation of hen lysozyme: A calorimetric and Raman study”, *J. Mol. Struct*., 891: 115–122.

[34] J. R. O’Donnell, A. K. Burnett, T. Sheehan, P. Tansey and G. A. McDonald (1981) “Safety of dimethylsulphoxide”. *Lancet*, 1**:** 8218.

[35] A. Zambelli, G. Poggi, G. A. Da Prada (1998) “Clinical toxicity of cryopreserved circulating progenitor cells infusion”. *Anticancer Res*.,18: 4705-4708.

[36] V. Antonenas, K. Bradstock, P. Shaw (2002) “Effect of washing procedures on unrelated cord blood units for transplantation in children and adults”, *Cytotherapy*, 4: 16.

[37] A. Martin, M. M. Bou-Ali, H. Barrutia, D. A. de Mezquia (2011) “Microfluidic separation process by the Soret effect in biological fluids”, *C. R. Mec*., 339: 342–348.

[38] S. Srinivasan, M. Ziad Saghir (2011), “Experimental approaches to study thermodiffusion - A review”, *International Journal of Thermal Sciences*, 50: 1125-1137.

[39] C. Ludwig, *Sitz. Ber. Akad. Wiss. Wien Math.-Naturw (1856)* Kl. 20:539.

[40] Ch. Soret (1879) “Une dissolution saline primitivement homogene”, *Archives des Sciences Physiques et Naturelles de Genève*. 3: 48-61.

[41] S. Van Vaerenbergh, A. Shapiro, G. Galliero, F. Montel, J. Legros, J. Caltagirone, J. Daridon and Z. Saghir (2005) “Multicomponent processes in crudes Benny Elmann-Larsen”, ESA SP-1290, ESTEC, Noordwijk, Netherlands: *ESA Publications Division*, ISBN 92-9092-971-5: 202 – 213.

[42] A. Firoozabadi, K. Ghorayeb, K. Shukla (2000) “Theoretical Model of Thermal Diffusion Factors in Multicomponent Mixutres”, *AIChE Journal, 46*: 892-900.

[43] R. T. Cygan and C. R. Carrigan (1992) “Time-Dependent Soret Transport: Applications To Brine And Magma”, *Chemical Geology*, 95: 201–212.

[44] F. Huang, P. Chakraborty, C. C. Lundstrom, C. Holmden, J. J. G. Glessner, S. W. Kieffer, C. E. Lesher (2010) "Isotope fractionation in silicate melts by thermal diffusion, *Nature*, 464: 396-400.

[45] D. Braun and A. Libchaber, (2004) "Thermal force approach to molecular evolution", *Phys. Biol.*, 1: 1-8.

[46] D. Braun and A. Libchaber (2002) "Trapping of dna by thermophoretic depletion and convection", *Phys. Rev. Lett.*, 89: 188103-188104.

[47] R. Piazza, S. Iacopiniab and B. Triulzi (2004) "Thermophoresis as a probe of particle–solvent interactions: The case of protein solutions", *Phys. Chem. Chem. Phys*., 6: 1616-1622.

[48] J. Janca, V. Kaspárková, V. Halabalová, L. Simek, J. Růzicka, E. Barosová (2007) "Micro-thermal field-low fractionation of bacteria", *J Chromatogr B Analyt Technol Biomed Life Sci.*, 852: 512-520.

[49] M. M. Bou-Ali, O. Ecenarro, J. A. Madariaga and C. M. Santamarıa, J. J. Valencia (2000) "Measurement of negative Soret coefficients in a vertical fluid layer with an adverse density gradient", *Phys. Rev. E*, 62 (1): 1420-1423.

[50] S. A. Putnam, D. G. Cahill, G. C. Wong (2007) Temperature Dependence of Thermodiffusion in Aqueous Suspensions of Charged Nanoparticles, *Langmuir*,.23 (18): 9221-9228.

[51] M. Braibanti, D. Vigolo and R. Piazza (2008) "Does thermophoretic mobility depend on particle size?", *PRL*, 100: 108303.

[52] J. Dutrieux, J.K. Platten, G. Chavepeyer, and M.M. Bou-Ali (2002) On the measuremente of positive Sotet coefficients, *J. Phys. Chem. B*, 106: 6104.

[53] J.J. Valencia, M.M. Bou-Ali, O. Ecenarro, J.A. Madariaga, C.M. Santamaría (2002) "Thermal nonequilibrium phenomena in fluid mixtures", in: S. Wiegand, W. Köhler (ed), *Lect. Notes Phys.*, *Springer, Berlin*, 584: 233–249.

[54] D. Alonso de Mezquia, M. M. Bou-Ali, M. Larranãga, J. A. Madariaga and C. Santamaría (2012) "Determination of molecular diffusion coefficient in n-alkane binary mixtures: empirical correlations", *J. Phys. Chem. B*, 116 (9): 2814-2819.

[55] Ansys Inc., (2010), Ansys-Fluent 13.0, Lebanon, USA

[56] Ansys inc., (2010), Gambit 2.4.6, Lebanon, USA

[57] P. Naumann, A. Martin, H. Kriegs, M. Larranaga, M. Mounir Bou-Ali and S. Wiegand (2012) "Development of a Thermogravitational Microcolumn with an Interferometric Contactless Detection System, *J. Phys. Chem. B*, 116: 13889−13897.

[58] C. L. Choy, K. W. Kwok, W. P. Leung, F. P. Lau (1994) "Thermal conductivity of poly (ether ether ketone) and its short-fiber composites", *J. Polym. Sci., Part B: Polym. Phys*., 32: 1389–1397.

[59] C. L. Choy, W. P. Leung (1990) “Thermal expansion of poly (etherether-ketone) (PEEK)”, J. Polym. Sci., Part B: Polym. Phys., 28:1965–1977.

[60] A. Mialdun, V. Yasnou, V. Shevtsova, A. Königer, W. Köhler, D. Alonso de Mezquia and M. M. Bou-Ali (2012) “A comprehensive study of diffusion, thermodiffusion, and Soret coefficients of water-isopropanol mixtures”, J Chem Phys. 24:136.

[61] K. Toda , Y. Ebisu , K. Hirota , S. Ohira S. (2012) “Membrane-based microchannel device for continuous quantitative extraction of dissolved free sulfide from water and from oil” Anal Chim Acta., 741:38-46.

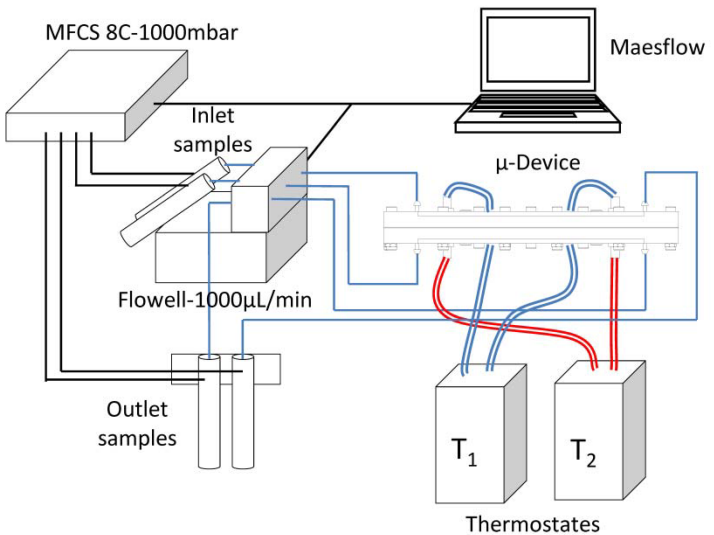
MFCS 8C-1000mbar
Maesflow
Inlet
samples
µ-Device
Flowell-1000µL/min
Outlet
samples
T1
T2
Thermostates

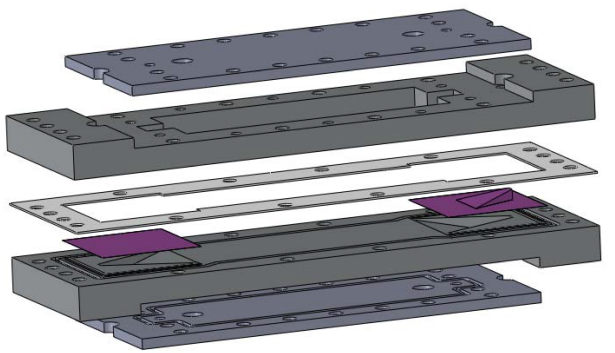

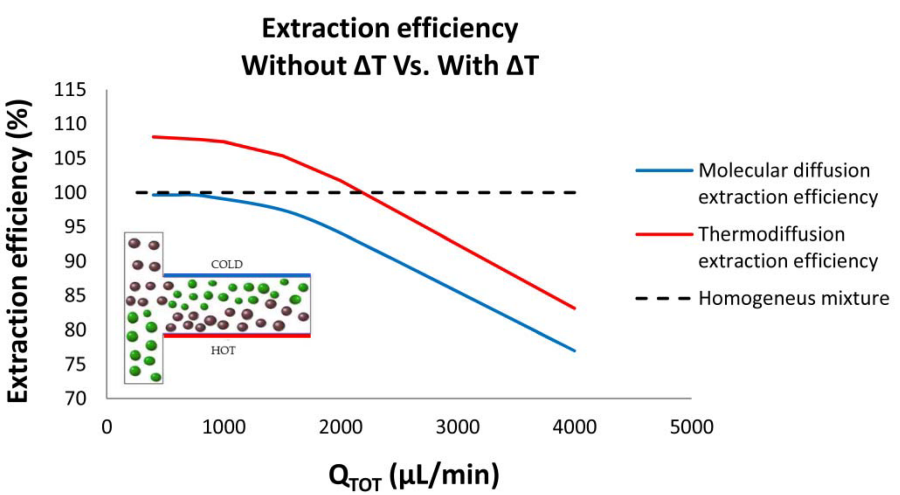
Extraction efficiency
Without ΔT Vs. With ΔT
Extraction efficiency (%)
115
110
105
100
95
90
85
80
75
70
0
1000
2000
3000
4000
5000
QTOT (µL/min)
COLD
HOT
Molecular diffusion
extraction efficiency
Thermodiffusion
extraction efficiency
Homogeneus mixture

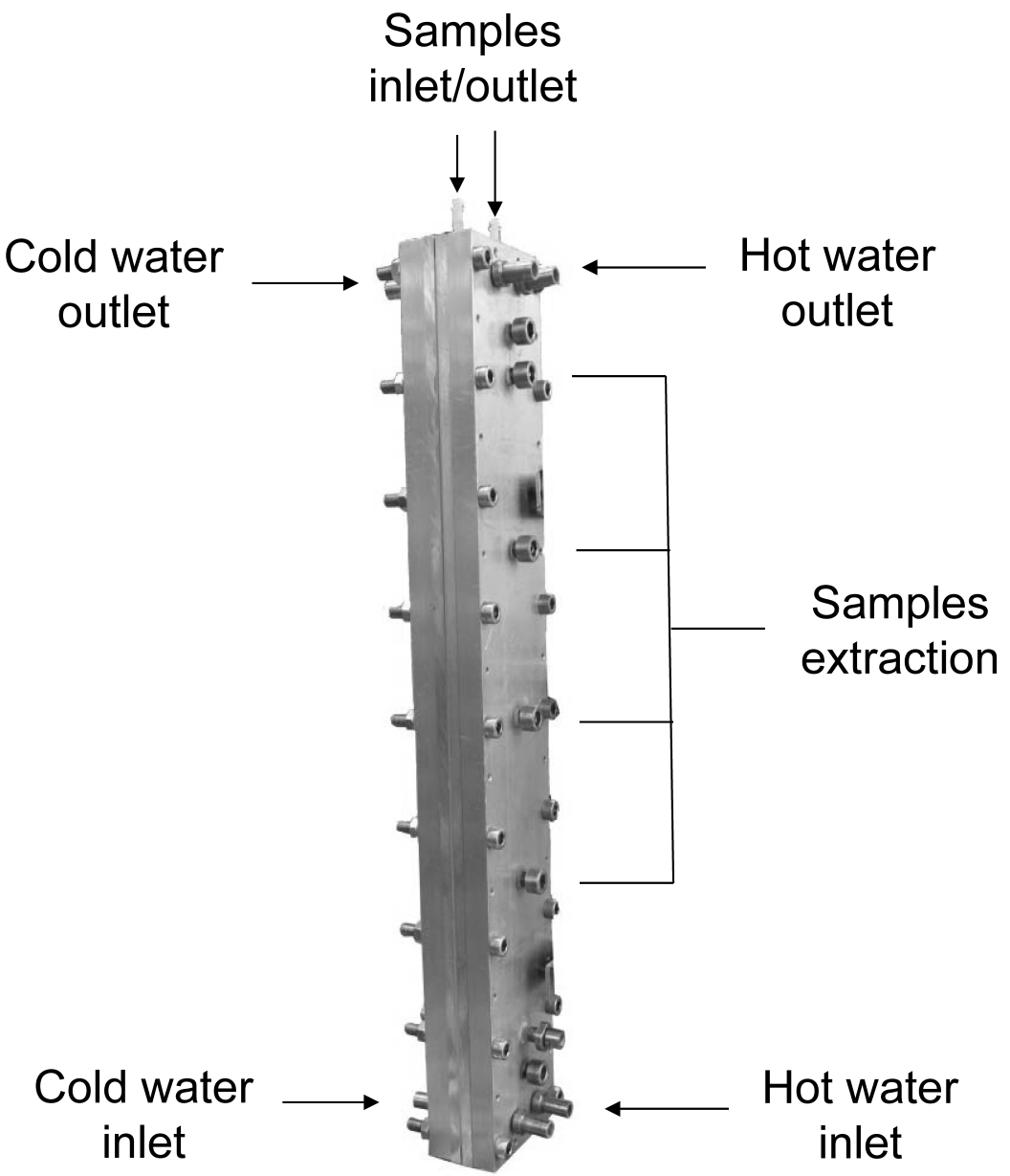
Samples
inlet/outlet
Cold water
outlet
Hot water
outlet
Samples
extraction
Cold water
inlet
Hot water
inlet

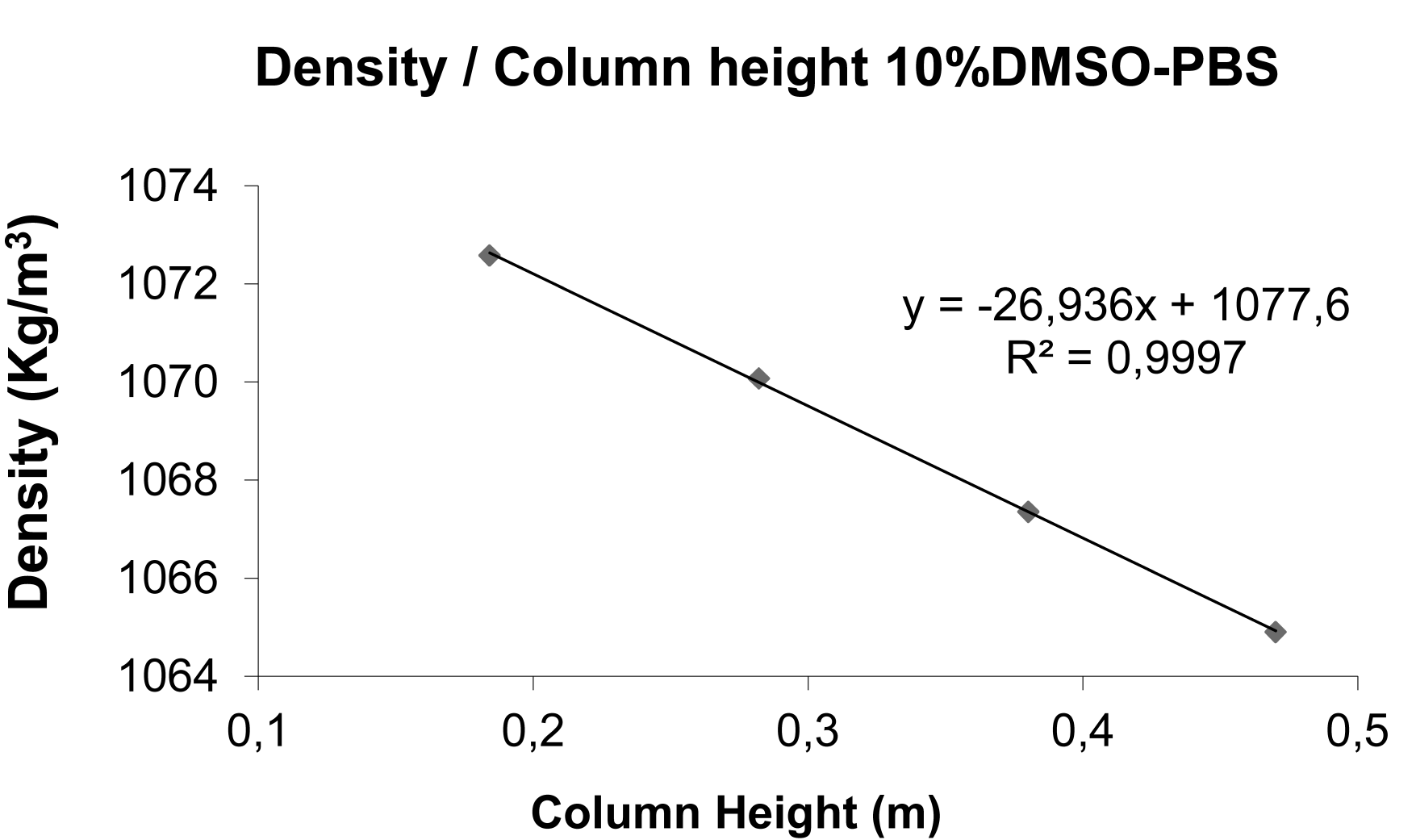
Density / Column height 10%DMSO-PBS
Density (Kg/m³)
1074
1072
1070
1068
1066
1064
y = -26,936x + 1077,6
R² = 0,9997
0,1
0,2
0,3
0,4
0,5
Column Height (m)

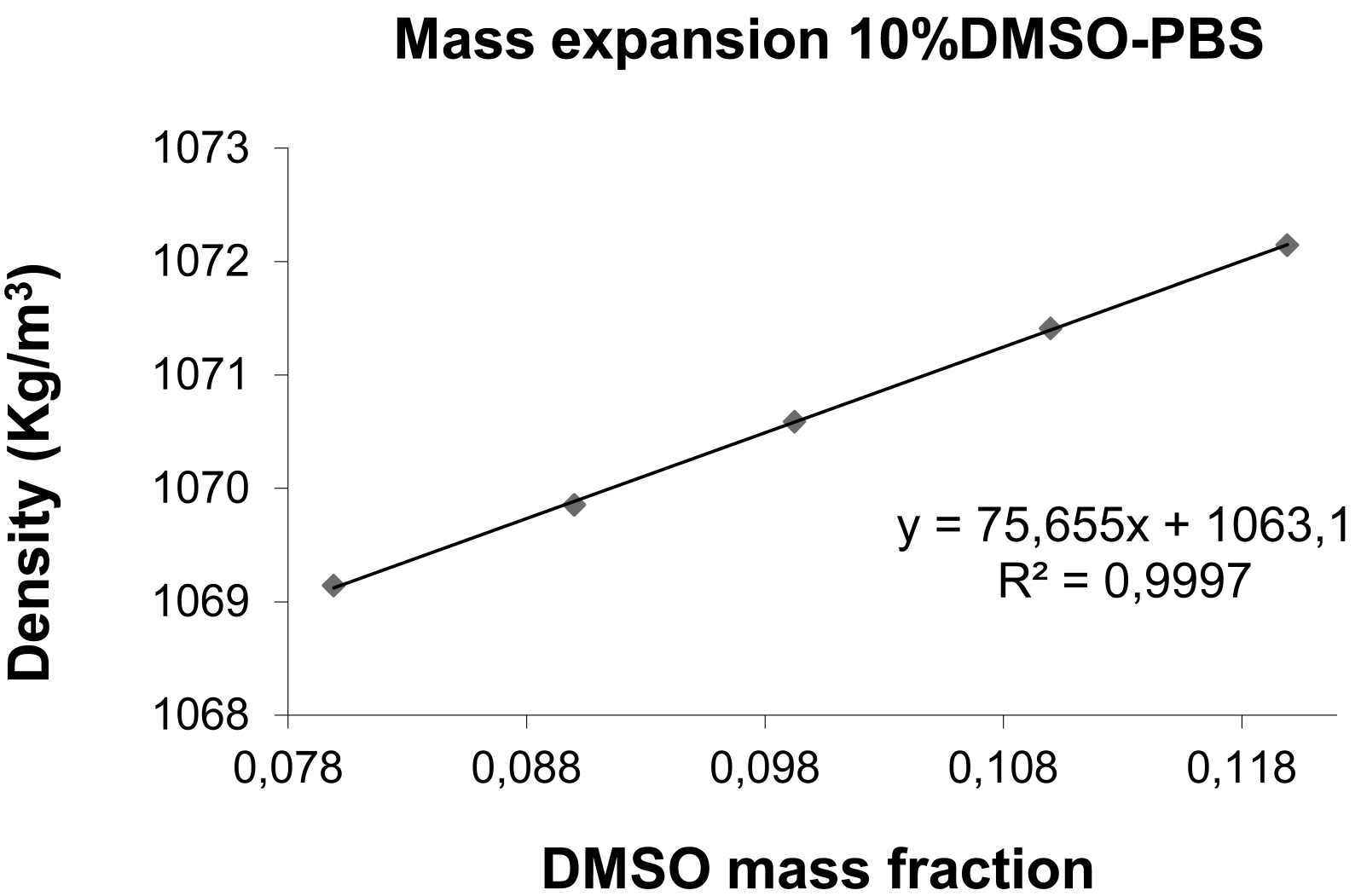
Mass expansion 10%DMSO-PBS
Density (Kg/m3)
1073
1072
1071
1070
1069
1068
0,078
0,088
0,098
0,108
0,118
y = 75,655x + 1063,1
R² = 0,9997
DMSO mass fraction

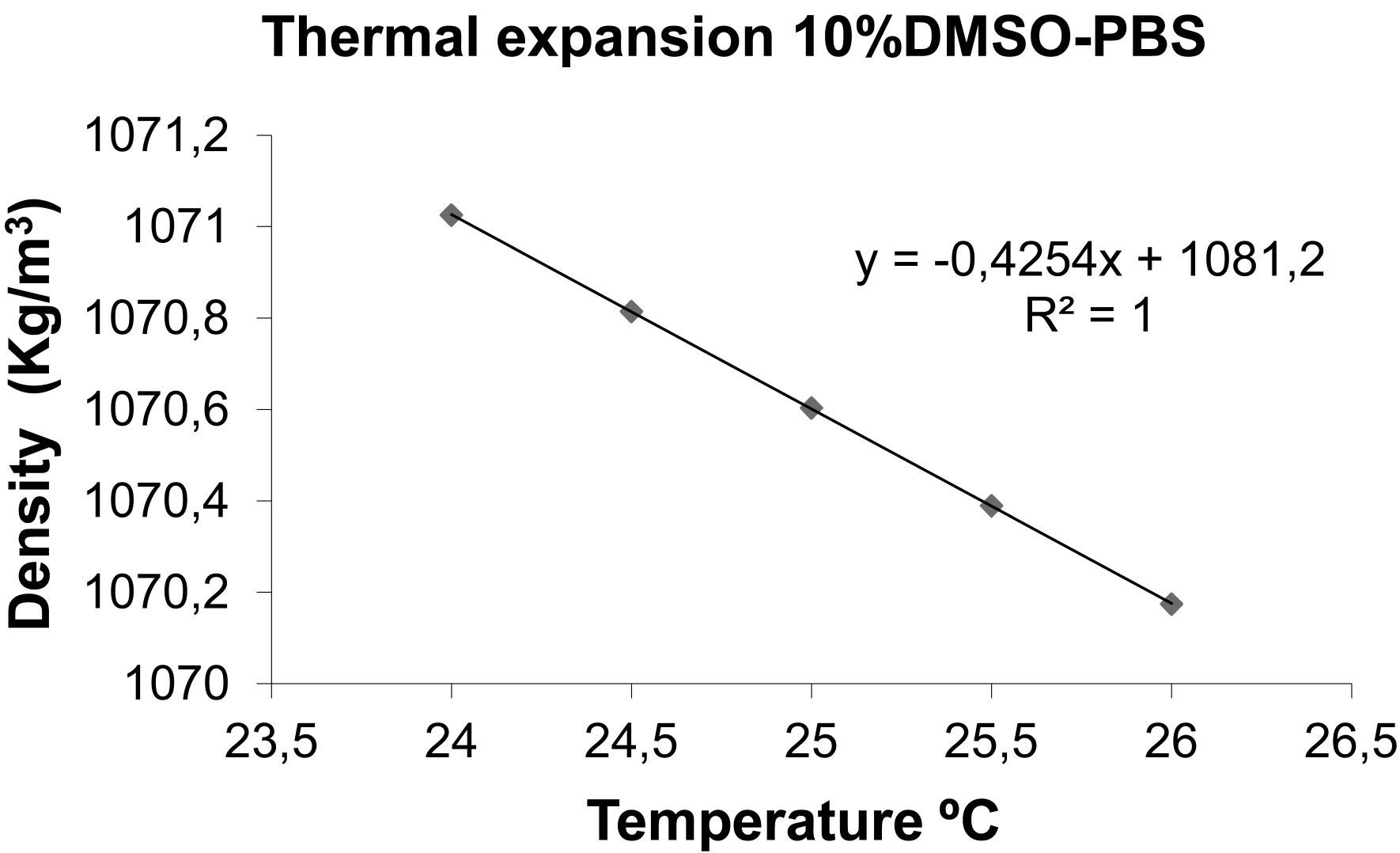
Thermal expansion 10%DMSO-PBS
Density (Kg/m³)
1071,2
1071
1070,8
1070,6
1070,4
1070,2
1070
y = -0,4254x + 1081,2
R² = 1
23,5
24
24,5
25
25,5
26
26,5
Temperature ºC

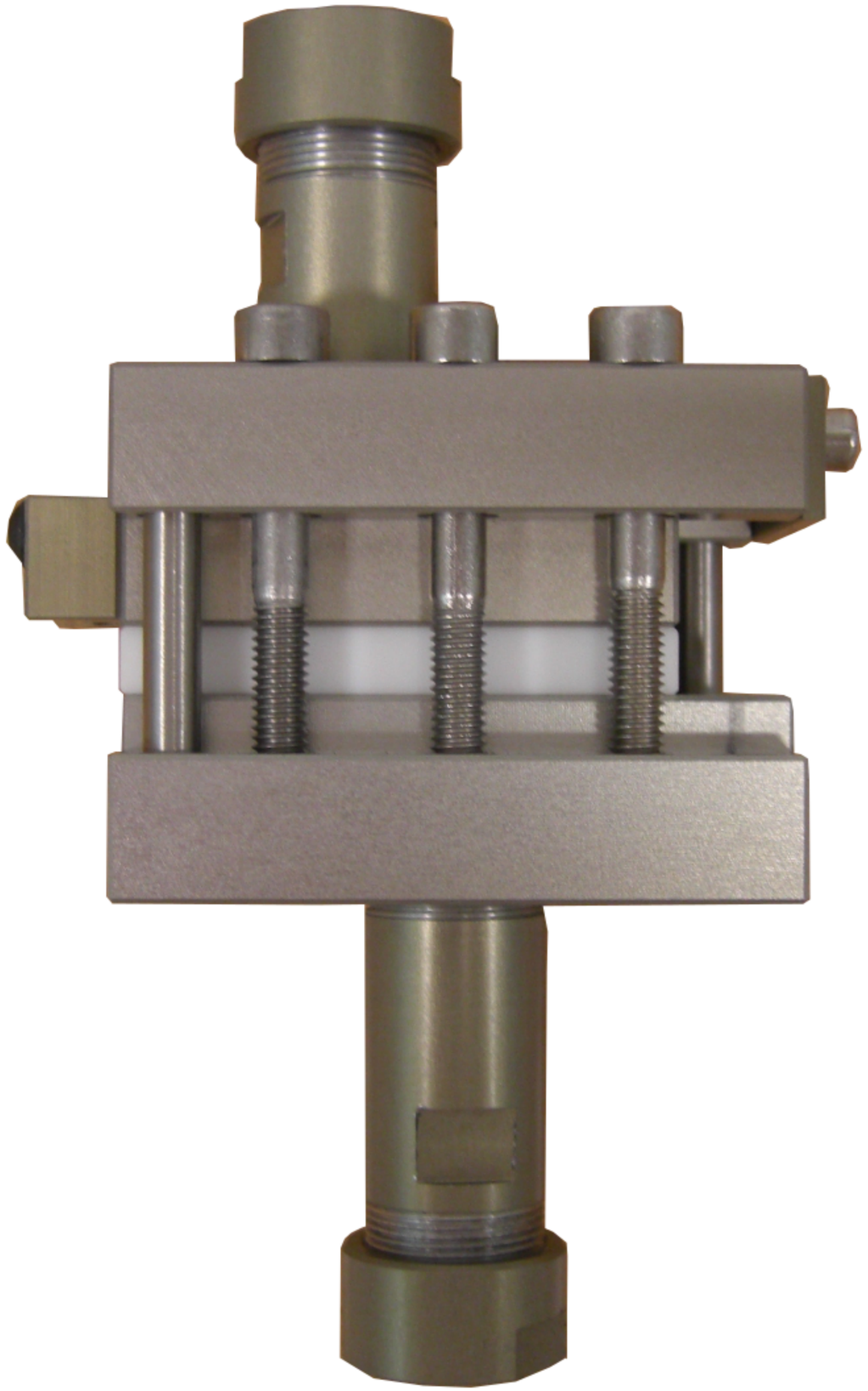

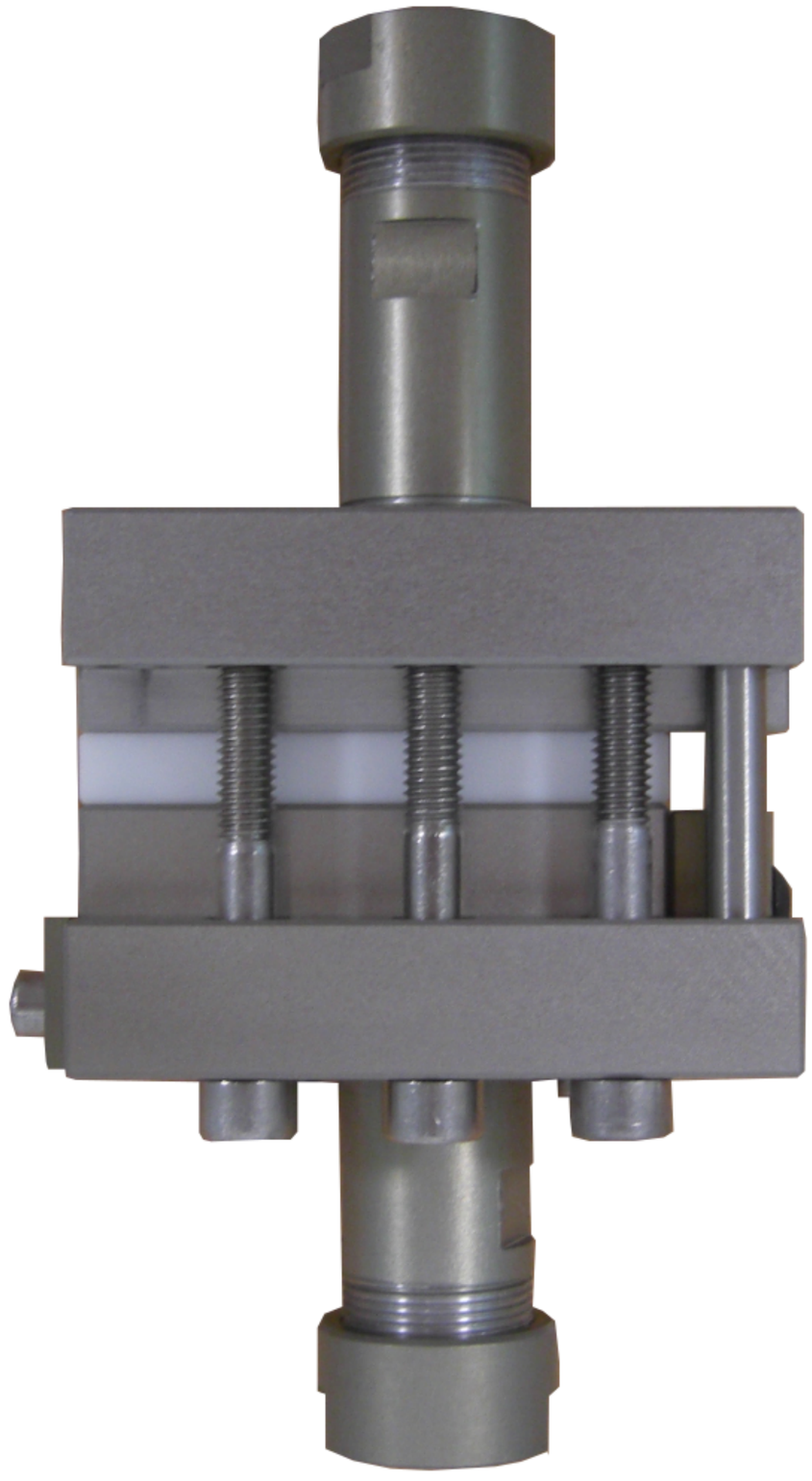

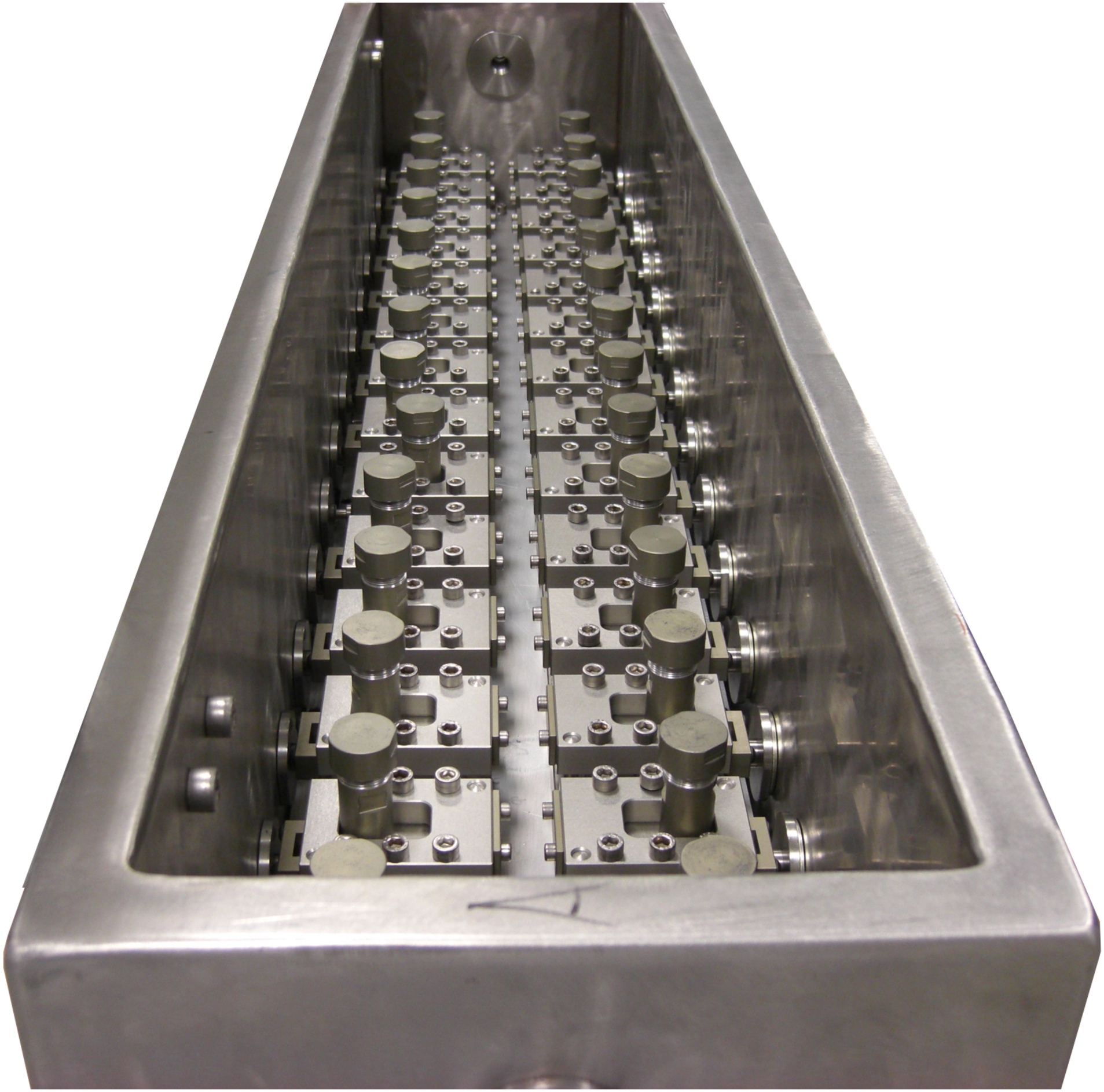

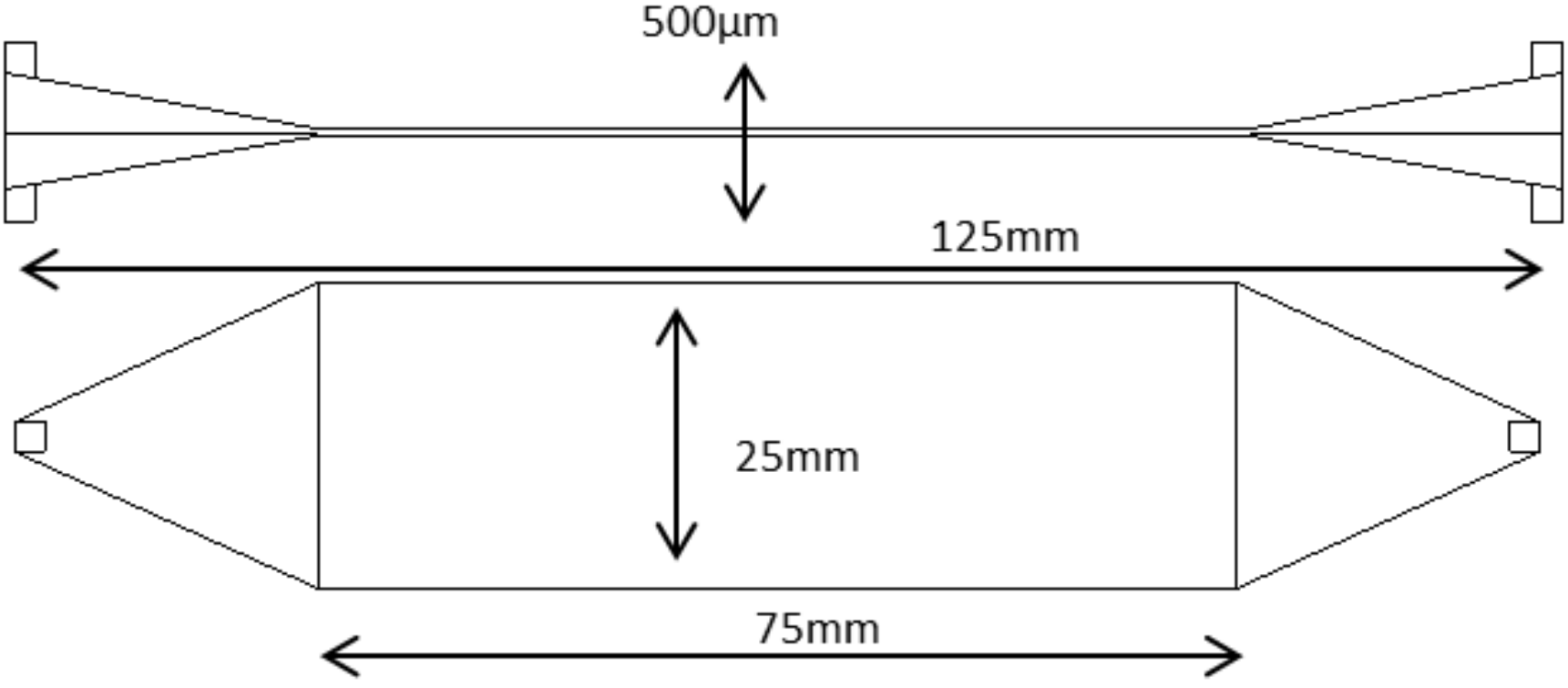
500µm
125mm
25mm
75mm

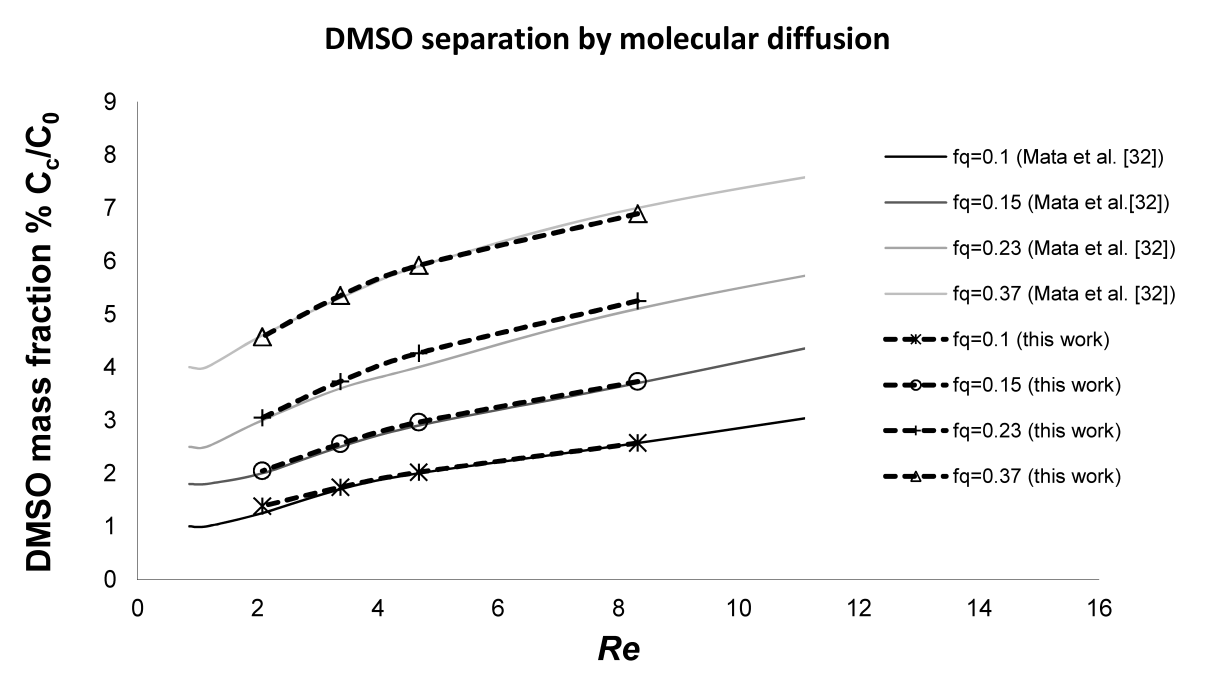
DMSO separation by molecular diffusion
DMSO mass fraction % C_c/C_0
Re
0
1
2
3
4
5
6
7
8
9
0
2
4
6
8
10
12
14
16
fq=0.1 (Mata et al. [32])
fq=0.15 (Mata et al.[32])
fq=0.23 (Mata et al. [32])
fq=0.37 (Mata et al. [32])
fq=0.1 (this work)
fq=0.15 (this work)
fq=0.23 (this work)
fq=0.37 (this work)

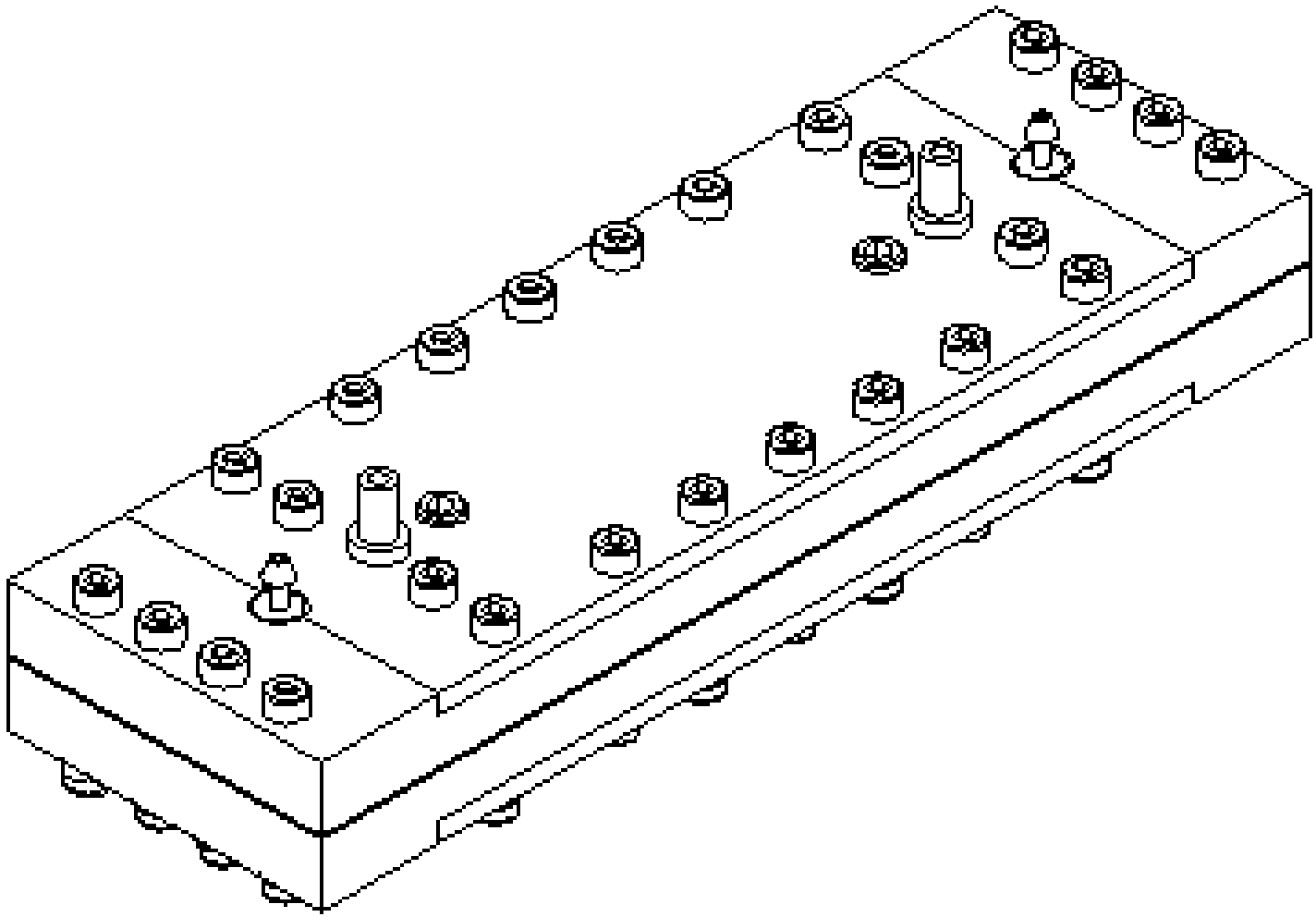

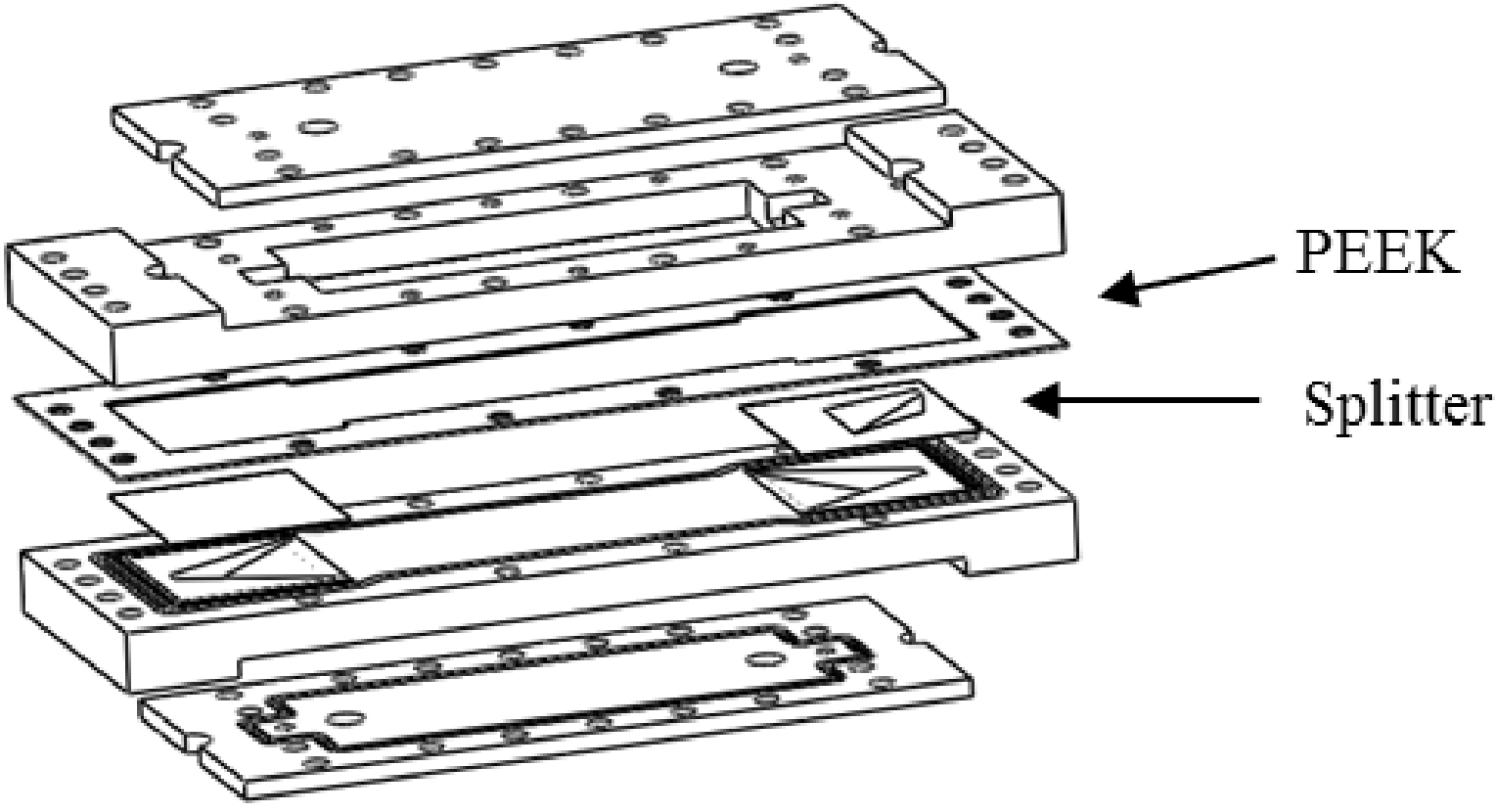
PEEK
Splitter

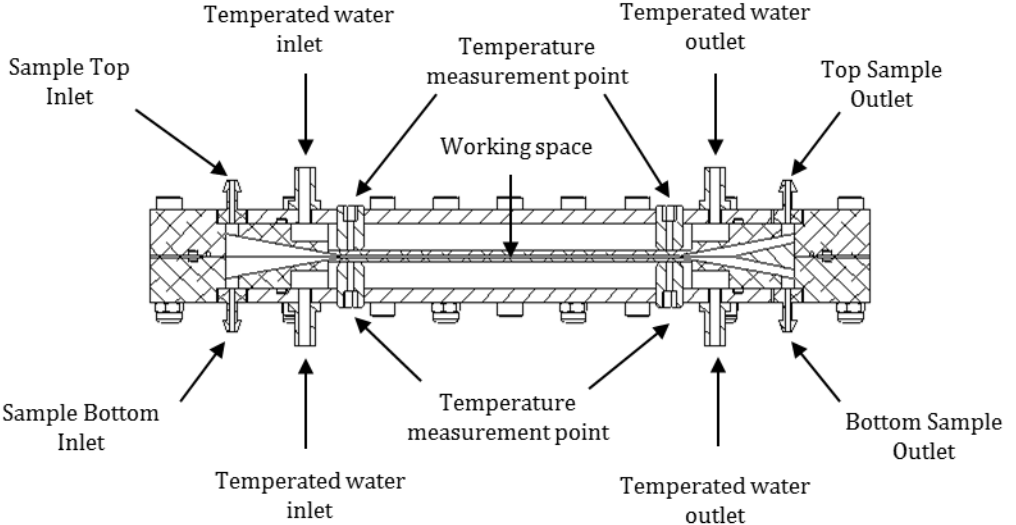
Temperated water inlet
Temperated water outlet
Sample Top Inlet
Temperature measurement point
Top Sample Outlet
Working space
Sample Bottom Inlet
Temperature measurement point
Bottom Sample Outlet
Temperated water inlet
Temperated water outlet

c)

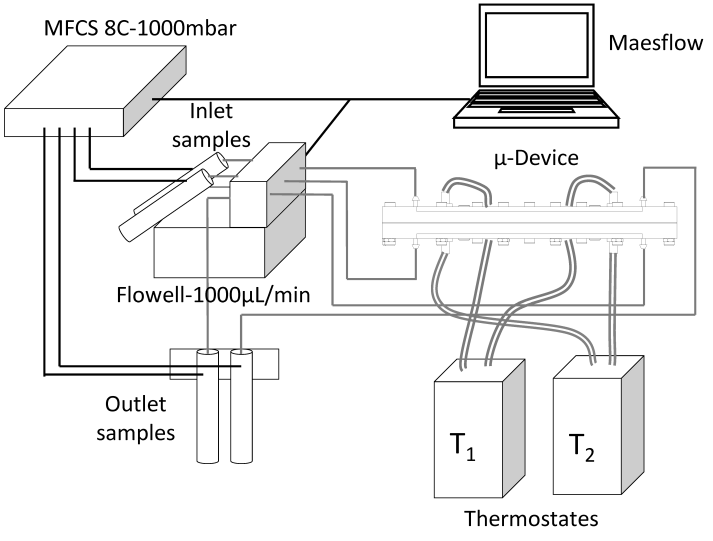
MFCS 8C-1000mbar
Maesflow
Inlet
samples
µ-Device
Flowell-1000µL/min
Outlet
samples
T1
T2
Thermostates

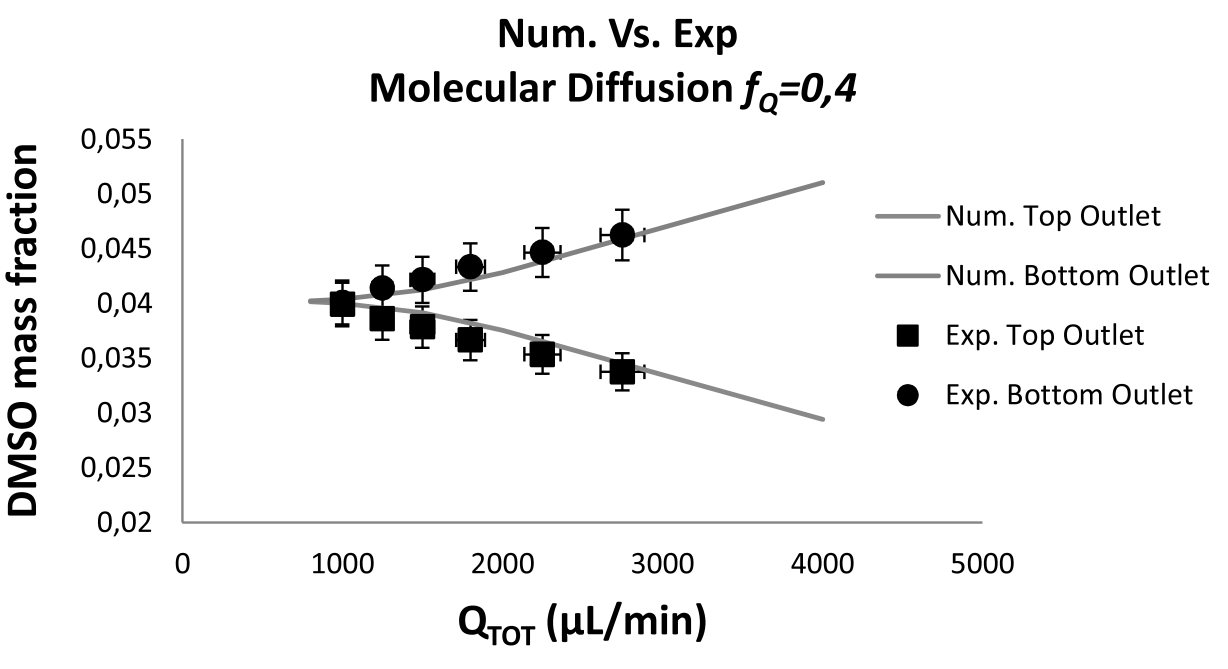
Num. Vs. Exp
Molecular Diffusion f_Q=0,4
DMSO mass fraction
0,055
0,05
0,045
0,04
0,035
0,03
0,025
0,02
0
1000
2000
3000
4000
5000
Q_{TOT} (µL/min)
Num. Top Outlet
Num. Bottom Outlet
Exp. Top Outlet
Exp. Bottom Outlet

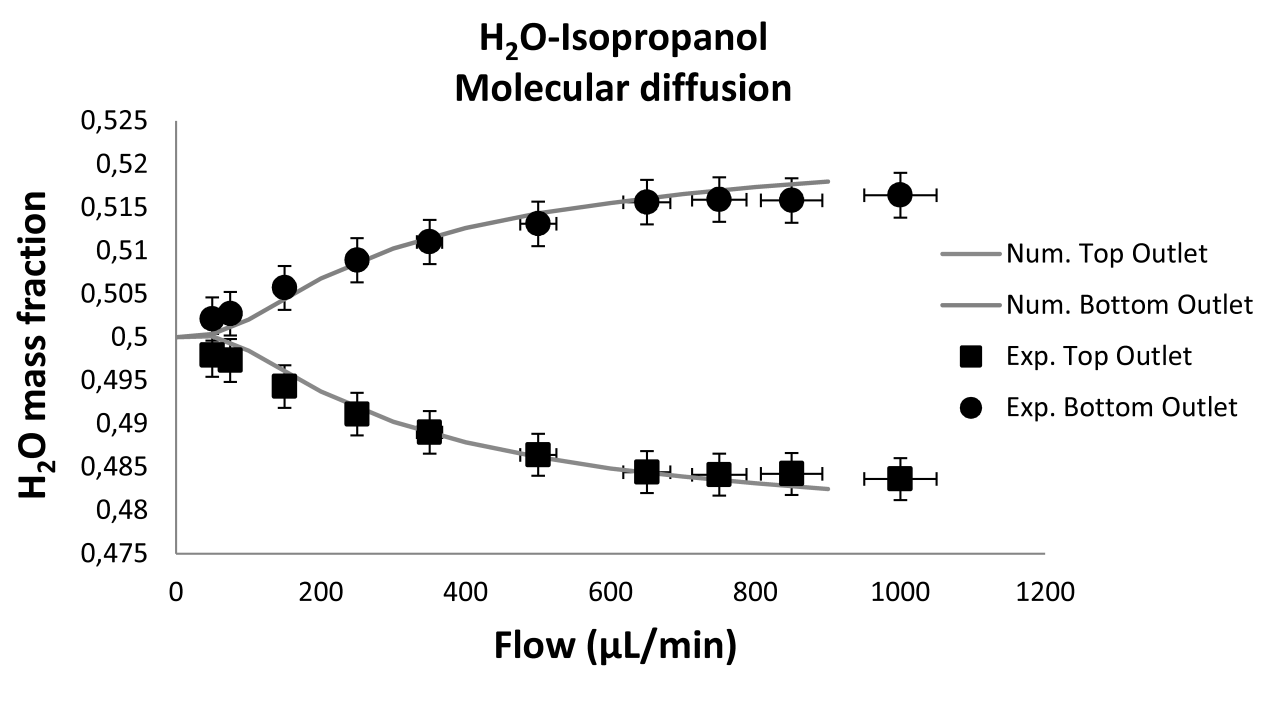
H2O-Isopropanol
Molecular diffusion
H2O mass fraction
0,525
0,52
0,515
0,51
0,505
0,5
0,495
0,49
0,485
0,48
0,475
0
200
400
600
800
1000
1200
Flow (µL/min)
Num. Top Outlet
Num. Bottom Outlet
Exp. Top Outlet
Exp. Bottom Outlet

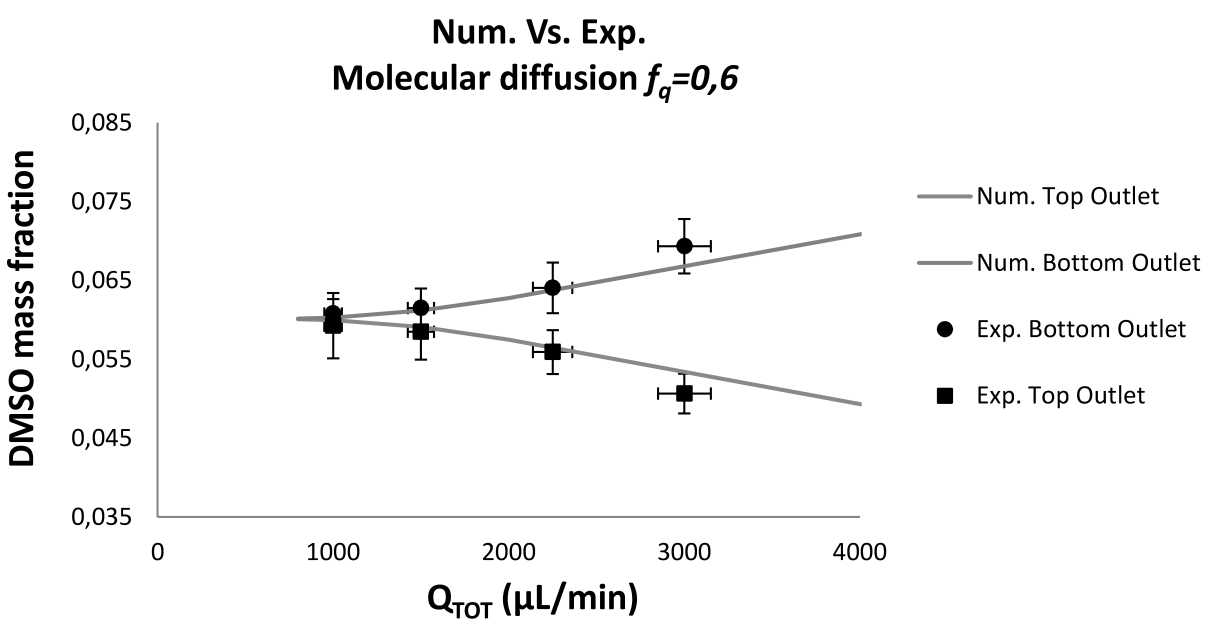
Num. Vs. Exp.
Molecular diffusion f_q=0,6
DMSO mass fraction
0,085
0,075
0,065
0,055
0,045
0,035
0
1000
2000
3000
4000
Q_{TOT} (µL/min)
Num. Top Outlet
Num. Bottom Outlet
Exp. Bottom Outlet
Exp. Top Outlet

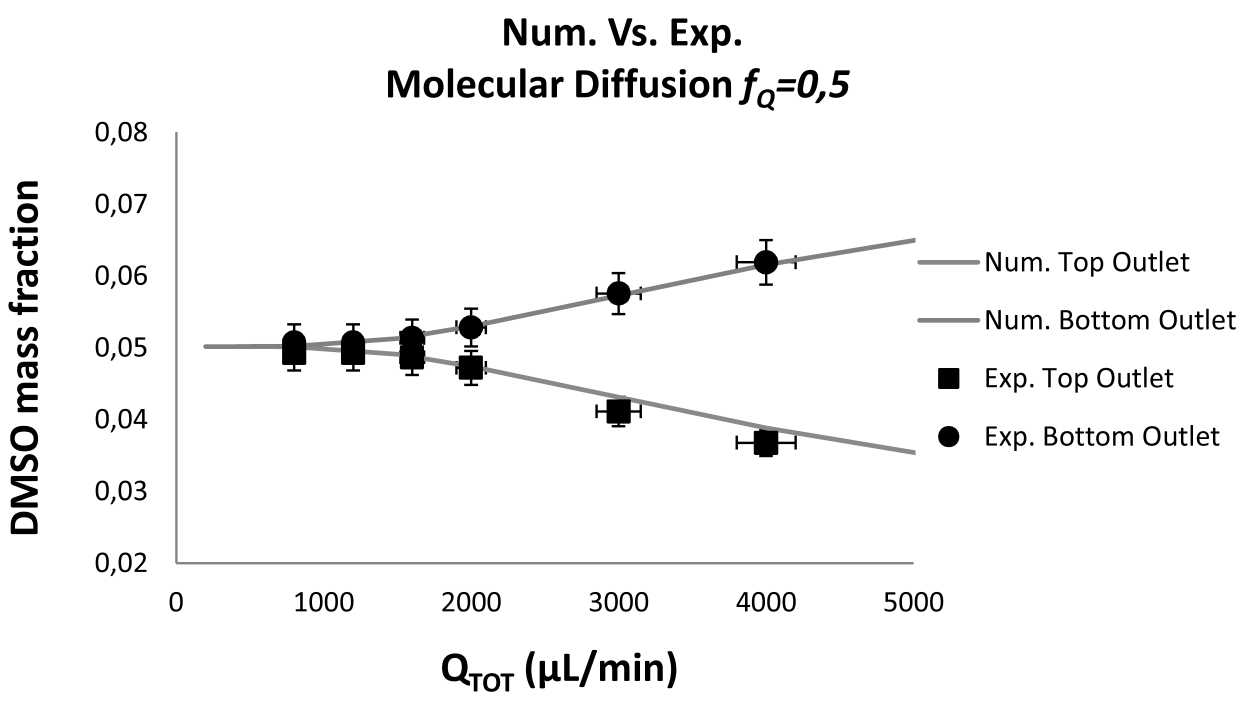
Num. Vs. Exp.
Molecular Diffusion f_Q=0,5
DMSO mass fraction
0,08
0,07
0,06
0,05
0,04
0,03
0,02
0
1000
2000
3000
4000
5000
Q_{TOT} (µL/min)
Num. Top Outlet
Num. Bottom Outlet
Exp. Top Outlet
Exp. Bottom Outlet

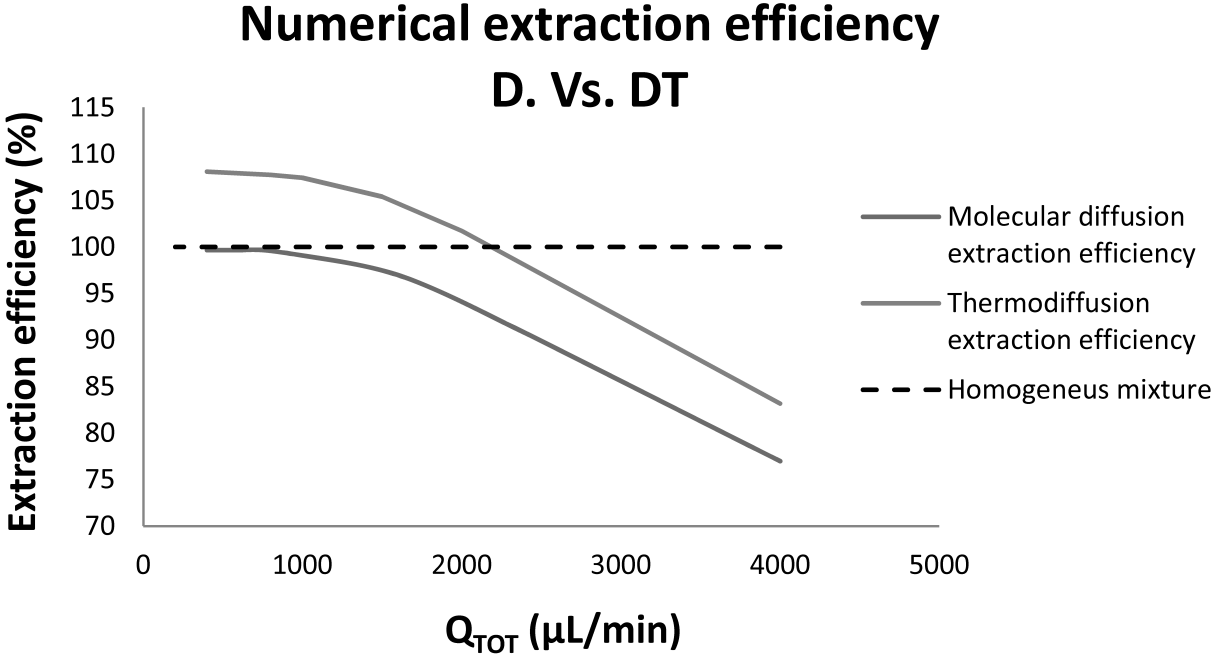
Numerical extraction efficiency
D. Vs. DT
Extraction efficiency (%)
115
110
105
100
95
90
85
80
75
70
0
1000
2000
3000
4000
5000
Q_{TOT} (µL/min)
Molecular diffusion extraction efficiency
Thermodiffusion extraction efficiency
Homogeneus mixture

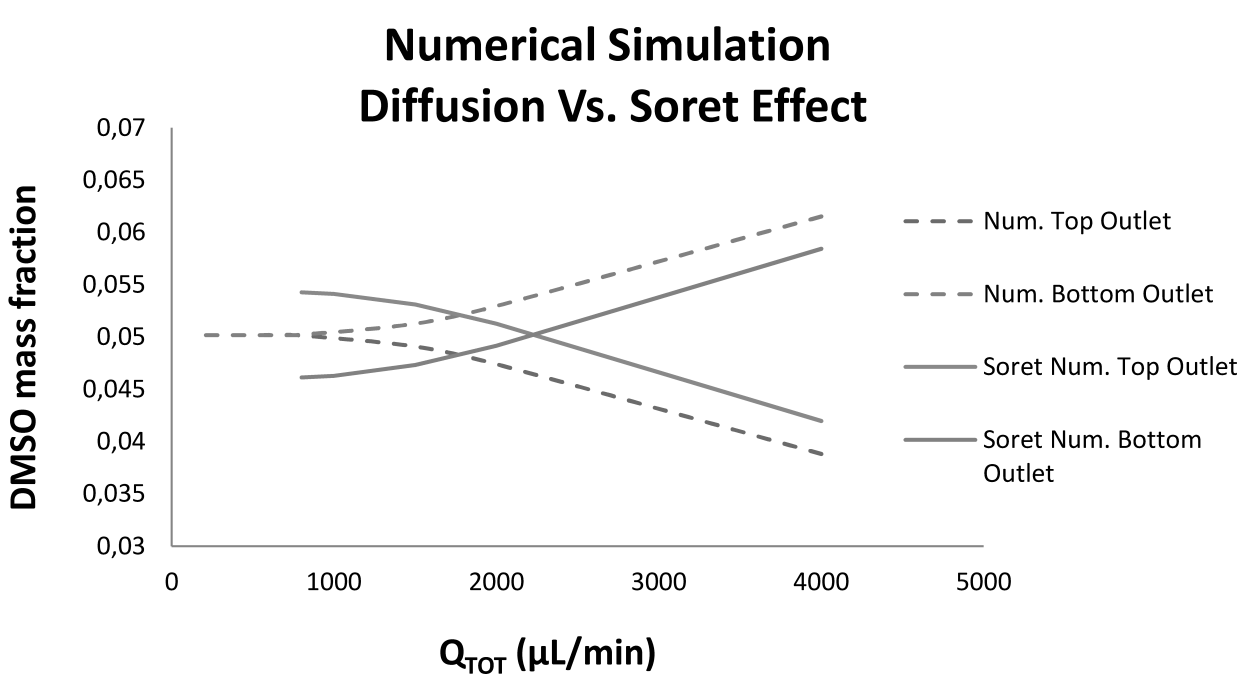
Numerical Simulation
Diffusion Vs. Soret Effect
DMSO mass fraction
0,07
0,065
0,06
0,055
0,05
0,045
0,04
0,035
0,03
0
1000
2000
3000
4000
5000
Q_{TOT} (µL/min)
Num. Top Outlet
Num. Bottom Outlet
Soret Num. Top Outlet
Soret Num. Bottom Outlet

Prof. Dr. Mounir Bou-Ali Saidi
mbouali@mondragon.edu
Mondragon Goi Eskola Politeknikoa
Loramendi 4, Apdo.23
20500 Mondragon
Spain

Prof. Dr. D. Gobin Editor-in-chief
Lab. EM2C, Ecole Centrale Paris
Grande Voie des Vignes
92295 Châtenay-Malabry, France

21th July 2016

Dear Prof. Dr. Gobin,

We would like to submit our manuscript entitled *"Optimizing Microfluidic Separation Processes By Thermodiffusion Effect" b*y Alain Martin-Mayor, M. Mounir Bou-Ali, Maialen Aginagalde and Pedro Urteaga to be considered for publication in the International Journal of Thermal Sciences for possible evaluation.

In this work, the great potential that thermodiffusion has on the improvement of the separation process in microdevices is demonstrated. In fact, applying a small temperature gradient (5K), an improvement of 10% in the separation process of an interesting mixture for biological purpose (10% DMSO/PBS) is achieved. Thus, to consider this effect could be key in applications at microscale, to use a temperature gradient coming from an external heat source, e.g., external actuator, in beneficial way for the process.

The separation process was analyzed both numerically and experimentally, for which it was necessary to construct and validate the microdevice, as well as determine experimentally the thermophysical and transport properties of the mixture of 10% of DMSO in PBS.

The following referees are suggested:

- Ellen K. Longmire, Department of Aerospace Engineering & Mechanics, University of Minnesota, Minneapolis, USA (longmire@umn.edu).
- Josef JancaJosef Janca, Institute of Scientific Instruments, Academy of Sciences of the Czech Republic, Brno, Czech Republic, (jjanca@ft.utb.cz).

- Stephane Colin, Clément Ader Institute, University of Toulouse, Toulouse, France, (stephane.colin@insa-toulouse.fr)

Thank you, in advance, for your consideration of this manuscript.
Yours sincerely,

Prof. Dr. M. Mounir Bou-Ali.

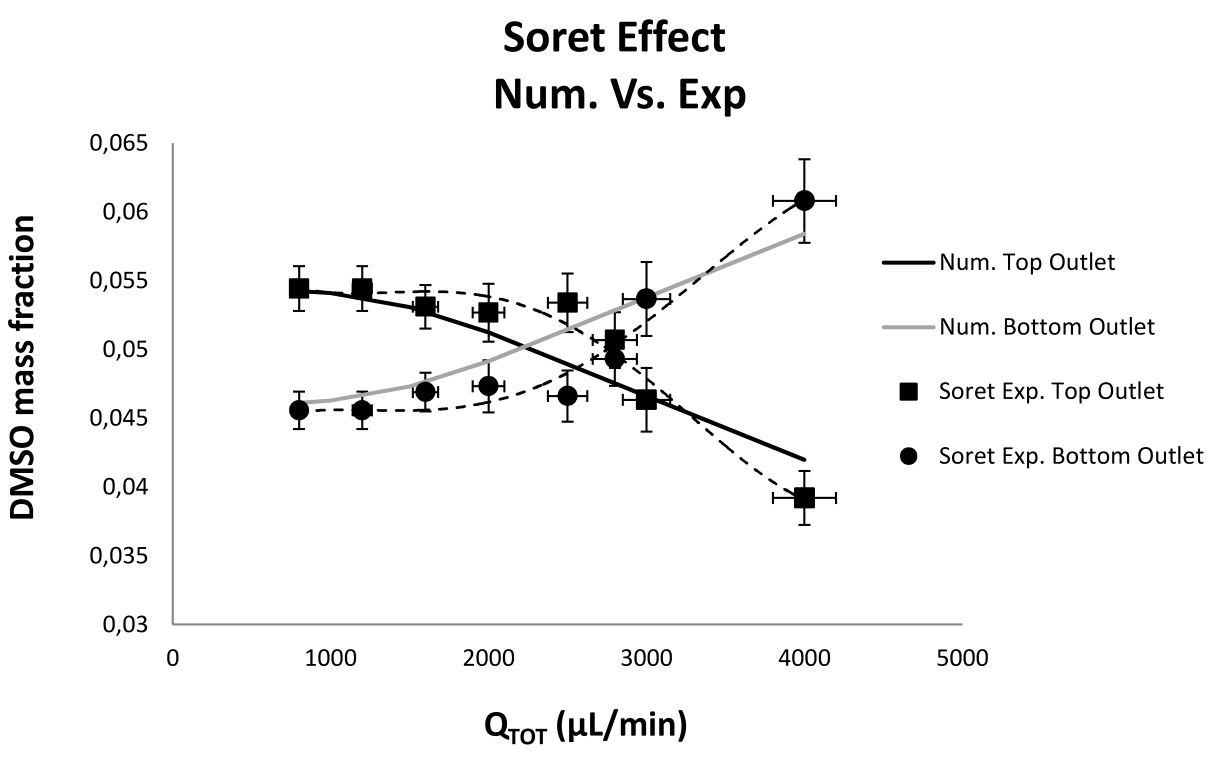
Soret Effect
Num. Vs. Exp
DMSO mass fraction
0,065
0,06
0,055
0,05
0,045
0,04
0,035
0,03
0
1000
2000
3000
4000
5000
Q_{TOT} (µL/min)
Num. Top Outlet
Num. Bottom Outlet
Soret Exp. Top Outlet
Soret Exp. Bottom Outlet